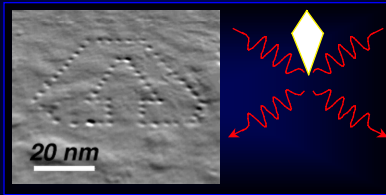# Introduction to XEDS in the AEM

20 nm

Nestor J. Zaluzec

zaluzec@microscopy.com

zaluzec@aaem.amc.anl.gov

Brief Review of X-ray Generation

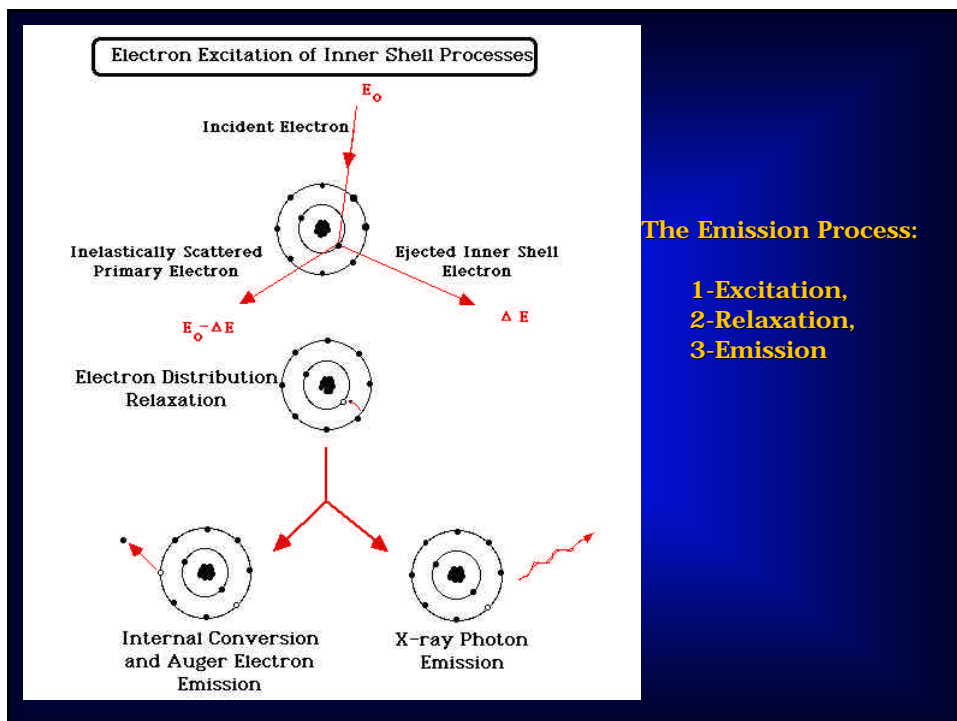Instrumentation: Detector Systems
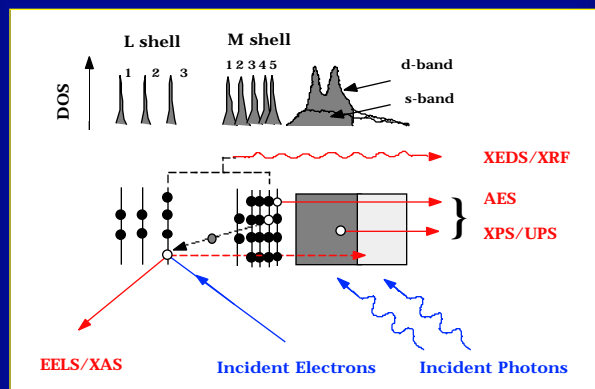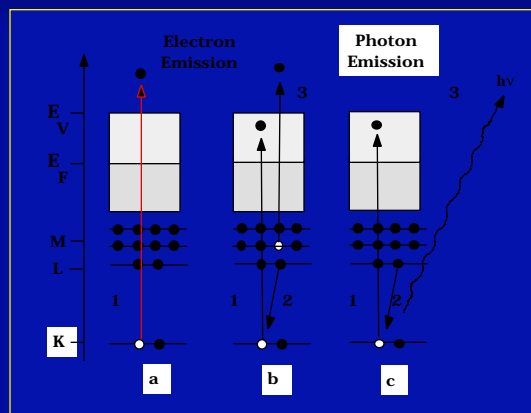
Instrumentation: EM Systems

Data Analysis and Quantification:

Additional Topics

Brief Review of X-ray Generation

Electron Excitation of Inner Shell & Continuum Processes
Characteristic and Bremsstrahlung Emission
Spectral Shapes
Notation of Lines

Electron Excitation of Inner Shell Processes

E_O

Incident Electron

Inelastically Scattered
Primary Electron

Ejected Inner Shell
Electron

$E_O - \Delta E$

ΔE

Electron Distribution
Relaxation

Internal Conversion
and Auger Electron
Emission

X-ray Photon
Emission

The Emission Process:

1-Excitation,
2-Relaxation,
3-Emission

2

Schematic Diagram Illustrating Sources of
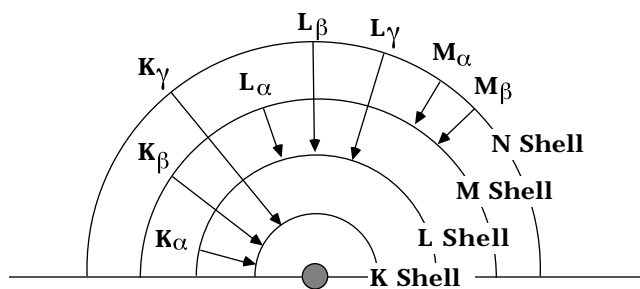Inelastic Scattering Signals

3

Experimental XEDS, XPS, and EELS data from the Copper L shell.
Note the differences in energy resolution, and spectral features.

Intensity (Arb Units)

XEDS

XPS

EELS

700   750   800   850   900   950   1000   1050   1100
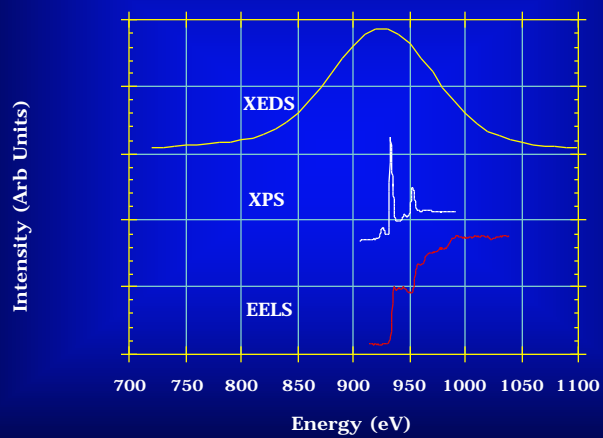
Energy (eV)

Nomenclature for Principle X-ray Emission Lines

L_β L_γ M_α

K_γ L_α M_β

K_β N Shell

M Shell

K_α L Shell

K Shell

Characteristic X-ray Line Energy   = E_{final} - $E_{initial}$

Recall that for each atom every shell has a unique energy level determined by

the atomic configuration for that element.

X-ray line energies are unique.
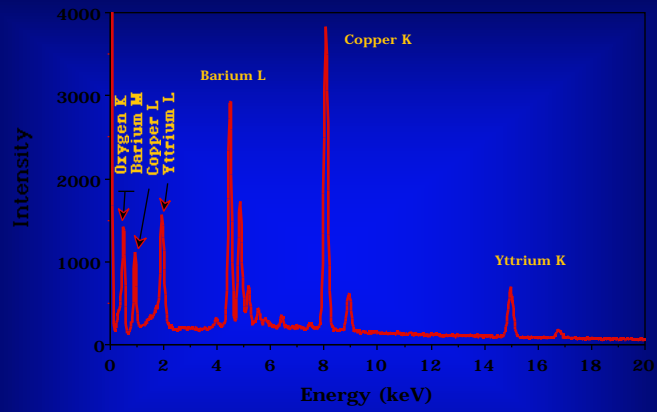
Nomenclature for X-ray Lines

X-ray Transition Selection Rules:
(Principle Quantum Numbers)

Shell	n	l	j	Rule
K	1	0	1/2	
L	2	0,1	1/2, 3/2	$\Delta n > 0$
M	3	0,1,2	1/2, 3/2, 5/2	$\Delta l = +1, -1$
N	4	0,1,2,3	1/2, 3/2, 5/2, 7/2	$\Delta j = +1, 0, -1$

Relative Intensities of Major X-ray Lines

$K_{\alpha 1} = 100$

$K_{\alpha 2} = 50$

$K_{\beta 1} = 15\text{-}30$

$K_{\beta 2} = 1\text{-}10$

$K_{\beta 3} = 6\text{-}15$

$L_{\alpha 1} = 100$

$L_{\alpha 2} = 50$

$L_{\beta 1} = 50$

$L_{\beta 2} = 20$

$L_{\beta 3} = 1\text{-}6$

$L_{\beta 4} = 3\text{-}5$

$L_{\gamma 1} = 1\text{-}10$

$L_{\gamma 3} = 0.5\text{-}2$

$L_{\eta} = 1$

$L_{\iota} = 1\text{-}3$

$M_{\alpha 1,2} = 100$

$M_{\beta} = 60$

Characteristic X-Ray Spectrum
Illustrating KLM lines

Intensity (4000, 3000, 2000, 1000, 0)

Copper K

Barium L

Oxygen K
Barium M
Copper L
Yttrium L

Yttrium K

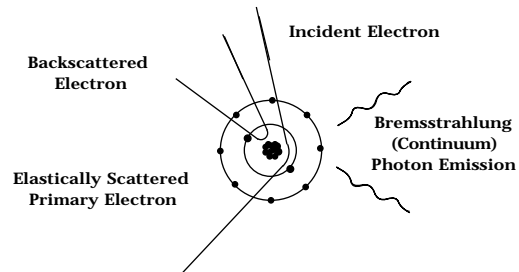Energy (keV) — 0, 2, 4, 6, 8, 10, 12, 14, 16, 18, 20
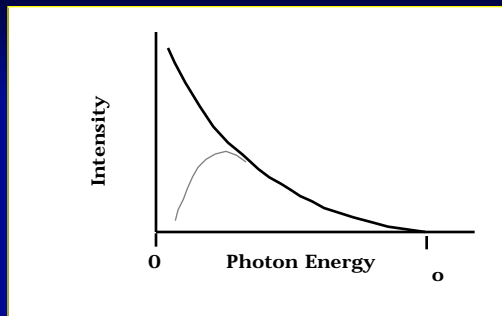
TEM Specimen: $Y_1Ba_2Cu_3O_{6.9}$ Superconductor - 120 kV - UTW Detector

Note:
        As Z increases the Kth shell line energy increases.
        If K-shell is excited then all shells are excited (Y, Cu,   Ba)
          but may not be detected.
        Severe spectral overlap may occur for low energy lines.


Electron Excitation of Continuum Processes

Incident Electron

Backscattered
Electron

Bremsstrahlung
(Continuum)
Photon Emission

Elastically Scattered
Primary Electron

6

Energy Range - Continuous Distribution

        Maximum = Incident Electron Energy (Least Frequent)
        Minimum = $E_{plasmon} \sim$ 15-30 eV (Most Frequent)

Spectral Distribution will reflect this range, modified by detector response function

---

Electron Excitation of Continuum (Background) Intensity
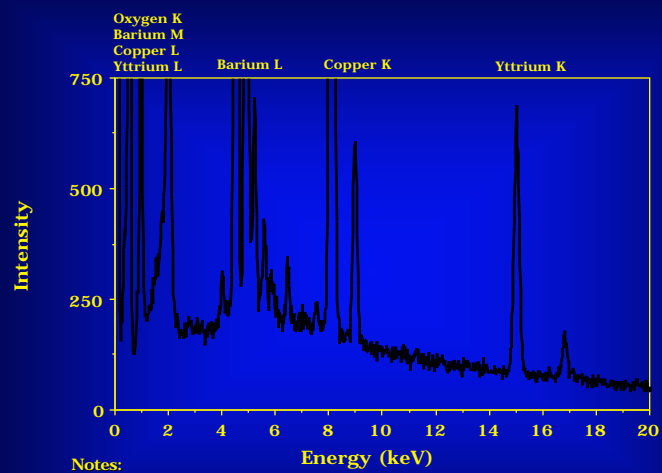
Notes:

    Spectral background will be influenced by:
        1.) Specimen composition
        2.) Detector efficiency
        3.) TEM generated artifacts

Instrumentation: Detector Systems

Wavelength Dispersive Spectrometers (WDS)
Energy Dispersive Spectrometers (EDS)
      Si(Li) Detectors
      HPGe Detectors
      Spectral Artifacts of the EDS System
      Detector Efficiency Functions
      Light Element Detectors
Multichannel Analyzers

Energy Dispersive Spectrometers: (Solid State Detector)

Operates on Energy Deposition Principle

Simple, Nearly Operator Independent
Large Solid Angles (0.05-0.3 sr)
Virtually Specimen Position Independent
No Moving Parts
Parallel Detection
Quantification by Standardless or Standards Methods

Poor Energy Resolution (~ 130 eV)
      ** SuperConducting Systems (~ 20 eV)
Poor Peak/Background Ratios (100:1)
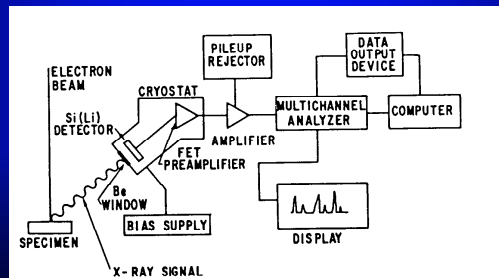Detection Efficiency Depends upon X-ray Energy

FIGURE 10. Operating schematic of a Si(Li) detector system.

Wavelength Dispersive Spectrometers : (Diffractometer)

Operates using Diffraction Principles (Bragg's Law)

Excellent Energy Resolution (~ 5 eV)
High Peak/Background Ratios (10000:1)
Good Detection Efficiency for All X-rays
High Counting Rates
Good Light Element Capabilities

Complex Mechanical Devices, Operator Intensive
Specimen Height dependant focus
Moving Components in the AEM
Limited Solid Angles (<0.01 sr)
Serial Detection
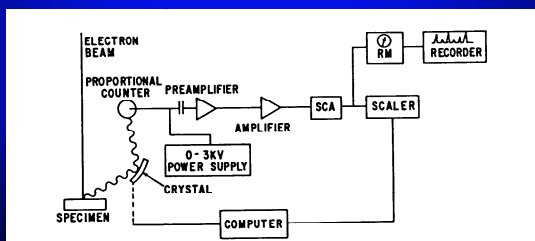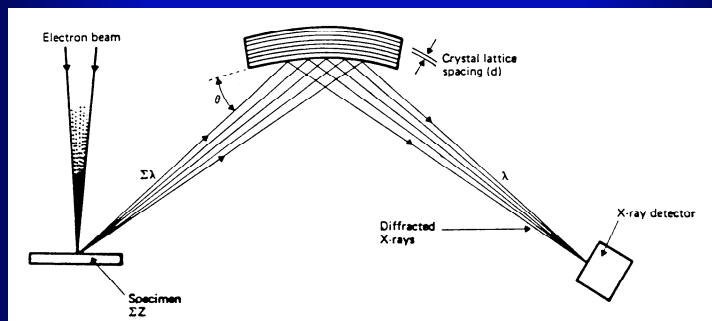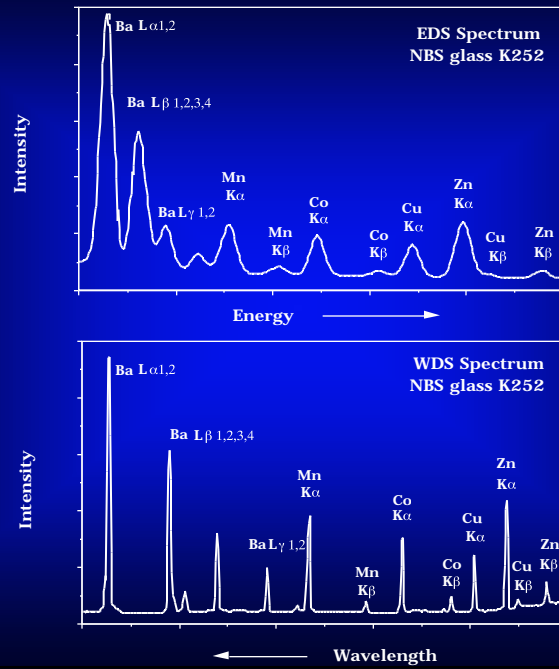Quantification Requires Standards

FIGURE 1. Basic components of a crystal diffraction spectrometer system.

Comparison of EDS and WDS Spectrometers

Parameter	Wavelength Dispersive	Energy Dispersive
Construction	Mechanical Device moving components	Solid State no moving parts
Energy Resolution	5 eV	130 eV
Efficiency	$\leq$ 30 %	100 % (3-15keV)
Input Count Rate	30-50 K cps	10 K cps
Peak/Background*	10000	100
Atomic Number Range	$Z \geq 4$ (Be)	$Z \geq 11$ (Na)
		$Z \geq 5$ (B)
Number of Elements	1 per Detector	All in Energy Range
Solid Angle	0.001-0.01 sr	0.02-0.3 sr
Collection Time	Tens of Minutes	Minutes
Beam Current	High Stability Required	Low Stability Required
Detector Stability	Good Short Term	Excellent
Spectral Artifacts	Neglegible	Important
Operation	Skilled (?)	Novice

* Values depend on definition, specimen, and operating conditions
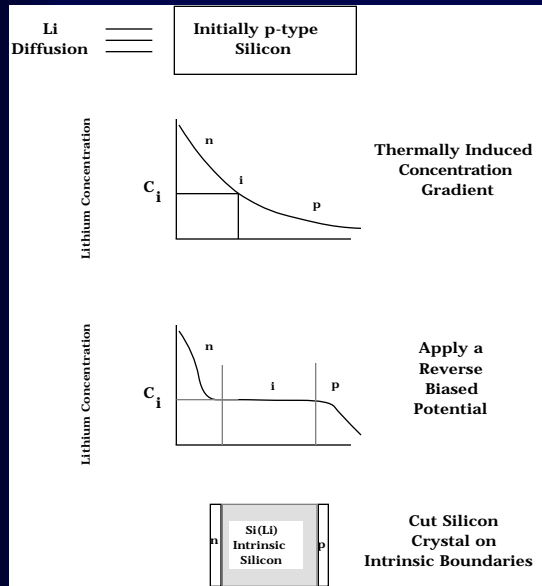
Comparison of EDS and WDS Spectra

**EDS Spectrum
NBS glass K252**

Intensity

Ba Lα1,2

Ba Lβ 1,2,3,4

Ba Lγ 1,2

Mn
Kα

Mn
Kβ

Co
Kα

Co
Kβ

Cu
Kα

Zn
Kα

Cu
Kβ

Zn
Kβ

Energy ⟶

**WDS Spectrum
NBS glass K252**

Intensity

Ba Lα1,2

Ba Lβ 1,2,3,4

Ba Lγ 1,2

Mn
Kα

Mn
Kβ

Co
Kα

Co
Kβ

Cu
Kα

Zn
Kα

Cu
Kβ

Zn
Kβ

⟵ Wavelength

Electron beam

Crystal lattice
spacing (d)

θ

Σλ

λ

Diffracted
X-rays

X-ray detector

Specimen
ΣZ

**Operation of a Crystal Spectrometer
Using Braggs' Law   = 2d sin ( )**

10
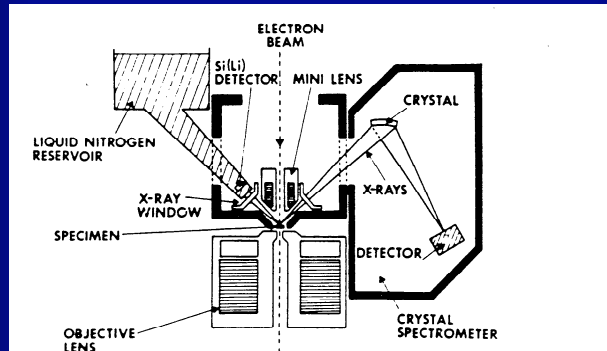
Installation of a Crystal Spectrometer in a
TEM - EMMA-4 System

Li Diffusion ▬▬ **Initially p-type Silicon**

Lithium Concentration

C_i n i p

Thermally Induced Concentration Gradient

Lithium Concentration

C_i n i p

Apply a Reverse Biased Potential

n | Si(Li) Intrinsic Silicon | p

Cut Silicon Crystal on Intrinsic Boundaries

• P-type Silicon high conductivity due to impurities (usually Boron); Lithium acts as a compensating dopant neutralizing the Si giving it a high resisitivity.

• Radiation deposits energy in the Si(Li) lattice & creates free electron-hole pairs in the crystal @ 1 electron-hole pair/3.8 eV of deposited energy @ 77K.

• Intrinsic semiconducting Si allows both electrons & holes to become mobile under application of a potential bias across the crystal

Properties of Intrinsic Silicon

.

Attaching HV electrodes to the two surfaces the Si(Li) crystal will act similiar to a capacitor with free charges developing on the electrical contacts. Charge developed in the crystal is N = E/ . (E= x-ray Energy, = 3.8 eV/e-h pair) i.e. ==> 10 kV X-ray produces ~2630 electrons = 4.2 x 10 -16 Coulombs.

Solid State Detector Construction
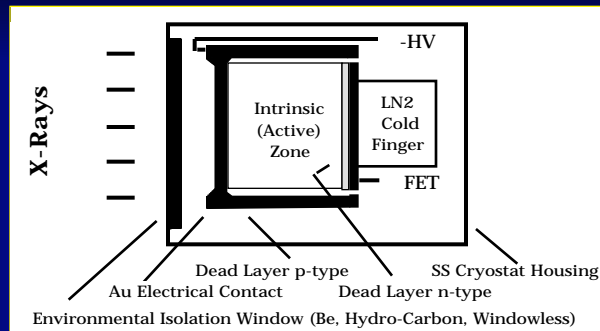
X-Rays

-HV

Intrinsic (Active) Zone

LN2 Cold Finger

FET

Dead Layer p-type
Au Electrical Contact
Dead Layer n-type
SS Cryostat Housing
Environmental Isolation Window (Be, Hydro-Carbon, Windowless)
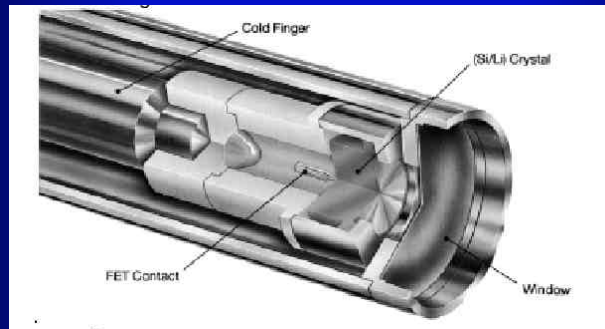
Relative Detection Efficiency

Solid State Detectors: Si(Li) or Instrinsic (High Purity) Ge
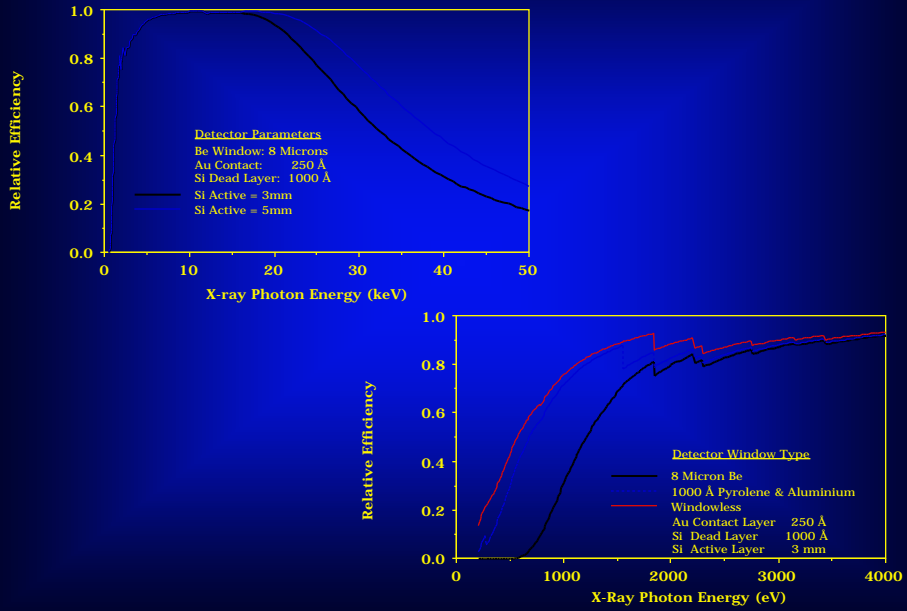Using a simple absorption model define the relative detector efficiency (E) by the following procedure:

$$I_T = I_o \exp(-\mu x) = I_o \exp\left(-\left[\frac{\mu}{\rho}\right]\rho\, x\right)$$

I_o x

Components of Si(Li) Detector

Relative Detection Efficiency

Solid State Detectors: Si(Li) or Instrinsic (High Purity) Ge
Using a simple absorption model define the relative detector efficiency (E)
by the following procedure:

$$I_T = I_o \exp(-\mu x) = I_o \exp\left(-\left[\frac{\mu}{\rho}\right]\rho\, x\right)$$

$$\varepsilon(E) = \frac{I_A * I_T}{I_o} = \exp\left(\sum_i^{HC/Be/Au/DL} -(\tfrac{\mu(E)}{\rho})_i * \rho_i * t_i\right) * \left\{1 - \exp\left(-(\tfrac{\mu(E)}{\rho})_j * \rho_j * t_j\right)\right\}$$

<--Absorption-->   <-- Transmission-->

$\frac{\mu(E)}{\rho}$ = mass absorption coefficient for Energy E; = density; t = layer thickness

**Calculated Si(Li) Detector Efficiency by Active Layer Thickness & Window Type**

Detector Parameters
Be Window: 8 Microns
Au Contact: 250 Å
Si Dead Layer: 1000 Å

Si Active = 3mm
Si Active = 5mm

X-ray Photon Energy (keV)

Relative Efficiency

Detector Window Type
8 Micron Be
1000 Å Pyrolene & Aluminium
Windowless
Au Contact Layer   250 Å
Si Dead Layer   1000 Å
Si Active Layer   3 mm

X-Ray Photon Energy (eV)

Relative Efficiency

Relative Transmission Efficiency

$$\varepsilon(E) = \frac{I_T}{I_o} = \exp\left(\sum_{i}^{Window} -\left(\frac{\mu(E)}{\rho}\right)_i * \rho_i * t_i \right)$$

$\underline{\mu(E)}$ = mass absorption coefficient for Energy E;   = density; t = layer thickness

Pyrolene N @1000Å
Diamond-Like C @ 0.4 µm
Aluminium @ 1000Å
B-90,N-9,H-1 @ 0.25 µm

Energy (eV)

Relative Transmission
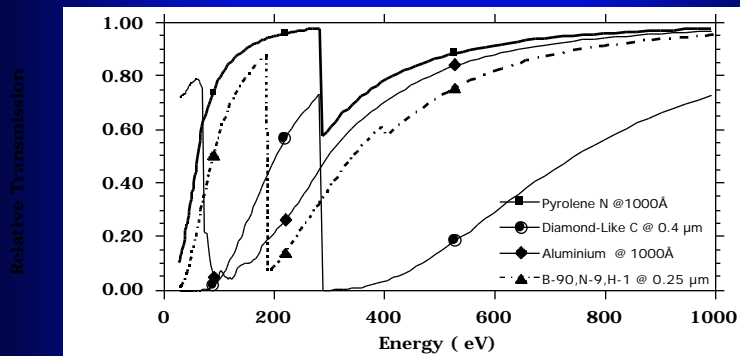
Note the Variation in transmission characteristics by Window Type.
Not all UltraThin Windows are Equivalent!!! For example Detection of Nitrogen
using a Diamond window is virtually impossible.

14

Windowless vs. Conventional Detectors
Comparision of XEDS measurement on NiO
using a Windowless versus Beryllium Window detector
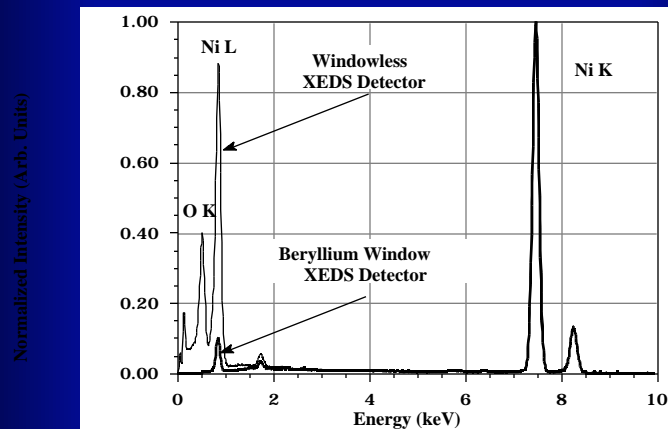
Note the enhanced detection efficiency below 1 keV for the WL detector. Both
spectra are normalized to unity at the Ni K α Line (7.48 keV)
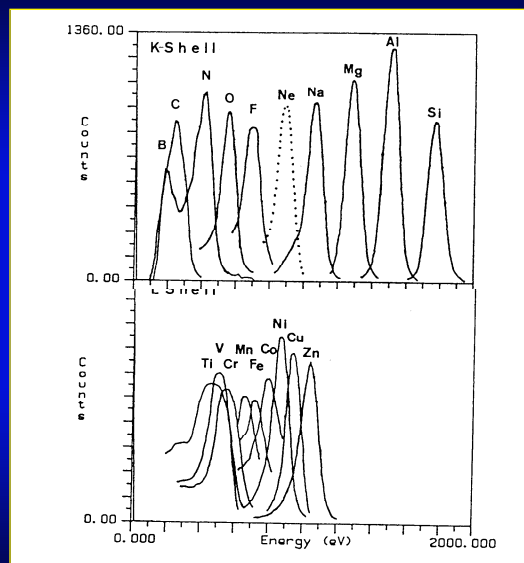
Windowless vs. Conventional Detectors

K Shell Spectra using
Windowless Detector

Boron -> Silicon
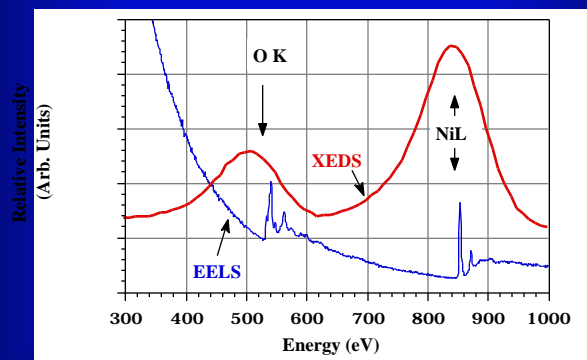
L Shell Spectra Using
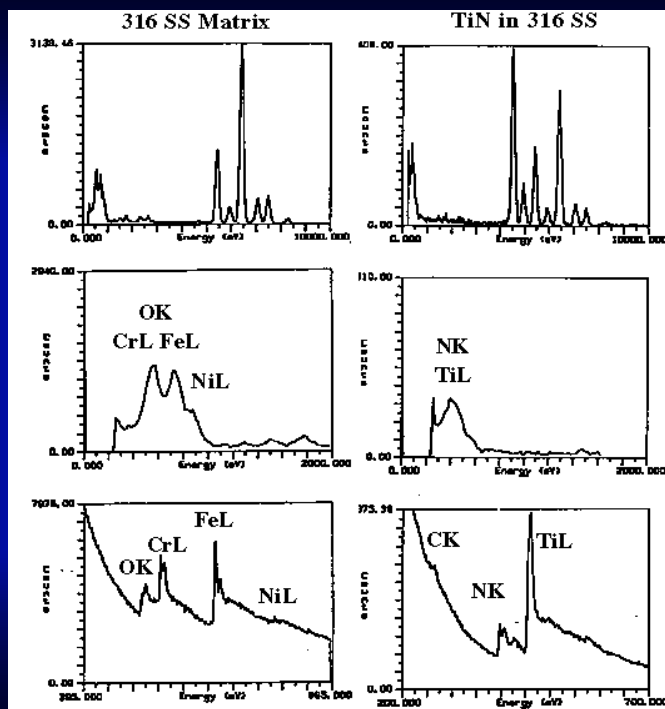Windowless Detector

Titanium ->Zinc

Note Potential Overlaps with
K shell Lines

**Comparision Light Element Spectroscopy
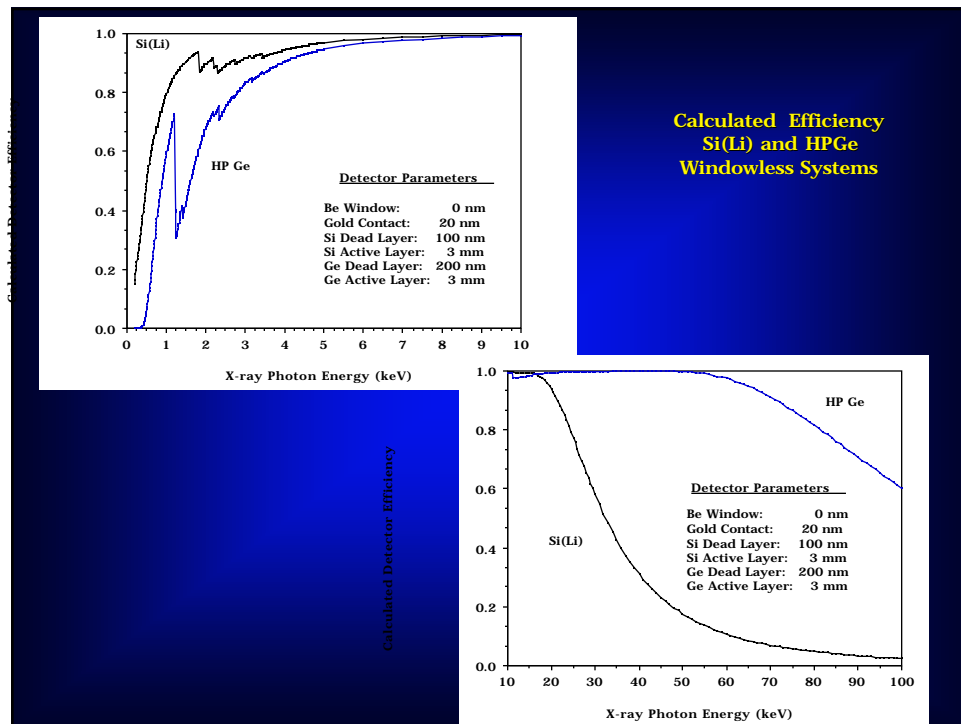Resolution XEDS vs EELS**

Comparision of WL XEDS Detector and EELS spectra
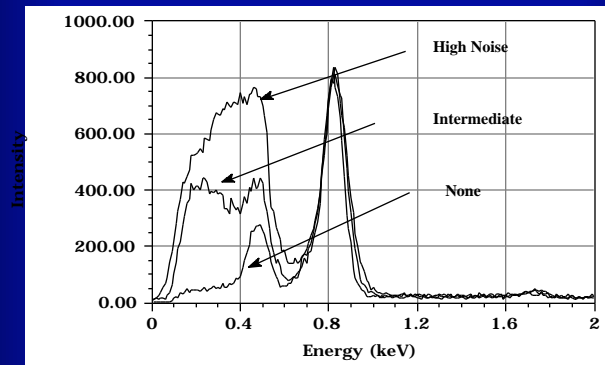taken from the same NiO specimen

Note the enhanced spectral information in the EELS data. Vertical
scale is arbitrary and chozen for clarity of presentation.

**Comparision
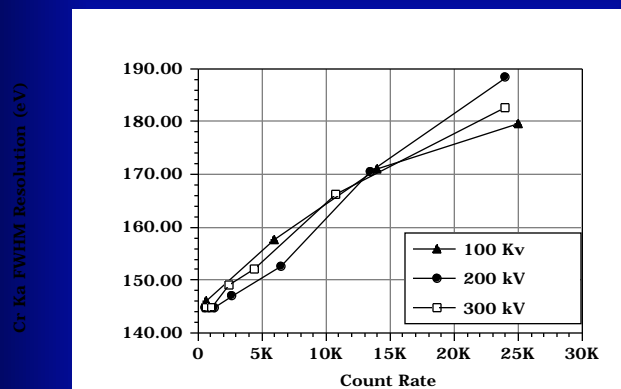Light
Element
Spectroscopy
Resolution
XEDS vs EELS**

Slide 1

Si(Li)

HP Ge

**Calculated Efficiency
Si(Li) and HPGe
Windowless Systems**

Detector Parameters

Be Window:	0 nm
Gold Contact:	20 nm
Si Dead Layer:	100 nm
Si Active Layer:	3 mm
Ge Dead Layer:	200 nm
Ge Active Layer:	3 mm

X-ray Photon Energy (keV)

Calculated Detector Efficiency

HP Ge

Si(Li)

Detector Parameters

Be Window:	0 nm
Gold Contact:	20 nm
Si Dead Layer:	100 nm
Si Active Layer:	3 mm
Ge Dead Layer:	200 nm
Ge Active Layer:	3 mm

X-ray Photon Energy (keV)

Slide 2

E_1 E_2 E_3 E_4 E_5 E_6 E_7

Counts

Microphonics

Distortion

Escape $E_4 - 1.74 \ keV$

Pile-Up $E_6 - \Delta E$

Sum $E_4 + E_4$

Sum $E_4 + E_5$

Energy (eV)

$$\text{Resolution} = \text{FWHM} = \sqrt{\text{Noise}^2 + 2.35^2 \varepsilon FE}$$

ε = 3.8 eV (in Si) / 2.9 eV (in Ge)
F = Fano Factor ~ 0.1
E = X-ray Energy
Noise = Electronic Noise (mainly in the FET)

Nominal FWHM Values in Modern Si(Li) Detectors:

O Kα (0.52 keV)	= 80 to 100 eV
Mn Kα (5.9 keV)	= 140 to 160 eV
Mo Kα (17.5 keV)	= 210 to 230 eV

**Resolution will also vary with
Microphonic & Electronic Noise, and Counting
Rate!**

WL & UTW detectors are particuliarly sensitive to low energy
noise and microphonics. Observe the changes in the spectra
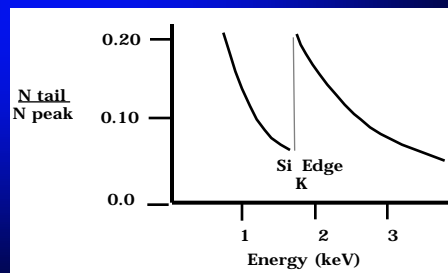
Resolution Loss with Count Rate

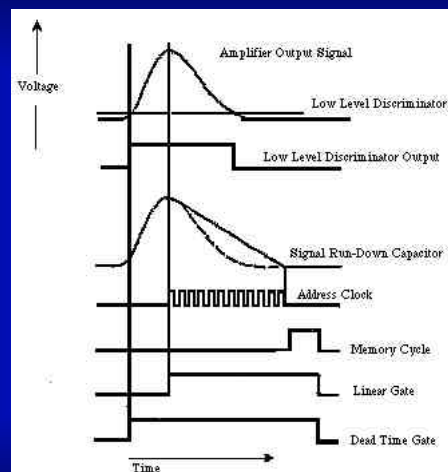## Incomplete Charge Collection in Solid State Detectors

Au Contact   **Si Dead Layer**

N_O —— $\eta < 1$ $\eta = 1$

d   **Si Active Layer**

$$N_{peak} = N_o \exp(-\mu d)$$

$$N_{tail} = N_o (1 - \exp(-\mu d))$$

$$\frac{N_{tail}}{N_{peak}} = \frac{(1 - \exp(-\mu d))}{\exp(-\mu d)}$$

$\frac{N\ tail}{N\ peak}$

0.20

0.10

0.0

Si Edge K

1   2   3

Energy (keV)
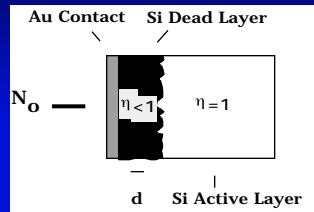
Operation of the Multi-Channel Analyzer

Voltage

Amplifier Output Signal

Low Level Discriminator

Low Level Discriminator Output

Signal Run-Down Capacitor

Address Clock

Memory Cycle

Linear Gate

Dead Time Gate

Time

Adapted from Gedcke, 1972

MCA/ADC Considerations
Detector Dead Time
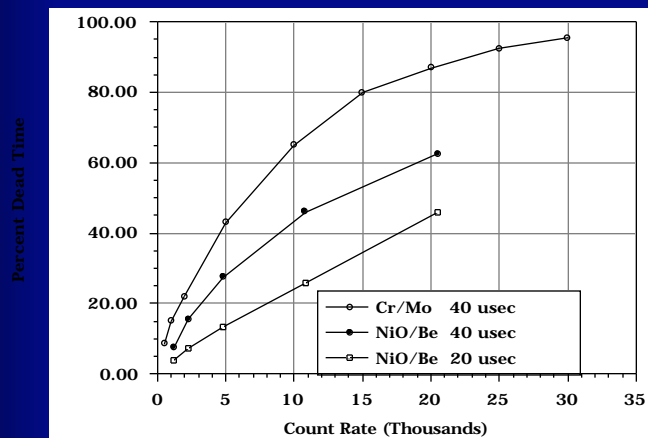
Instrumentation: AEM Systems

The AEM as a system
Spectral Artifacts in the AEM
      Uncollimated Radiation
      Systems Peaks
      Artifacts at High Electron Energy
Specimen Contamination & Preparation
Optimizing Experimental Conditions

Spectral Artifacts in the AEM
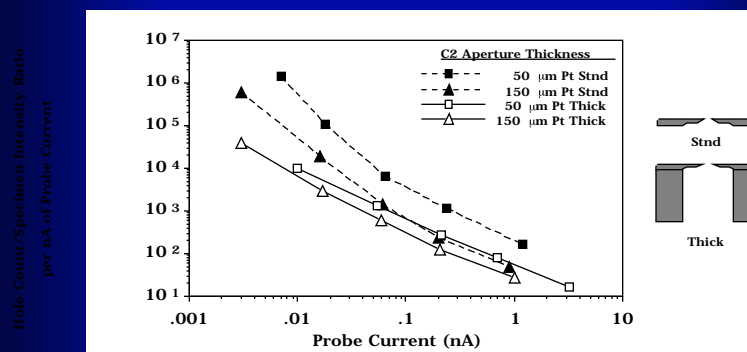**Uncollimated Radiation: The Hole Count**
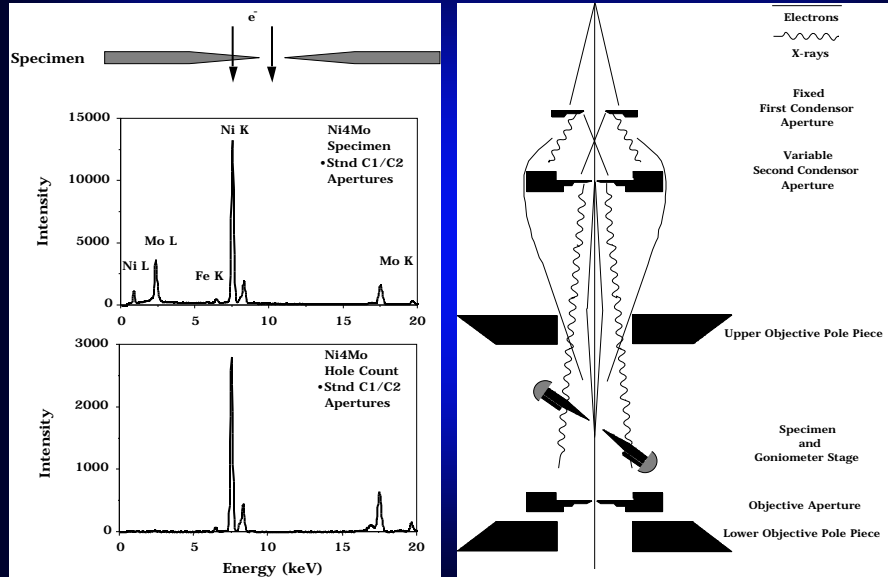
Spectral Artifacts in the AEM
Uncollimated Radiation Solutions
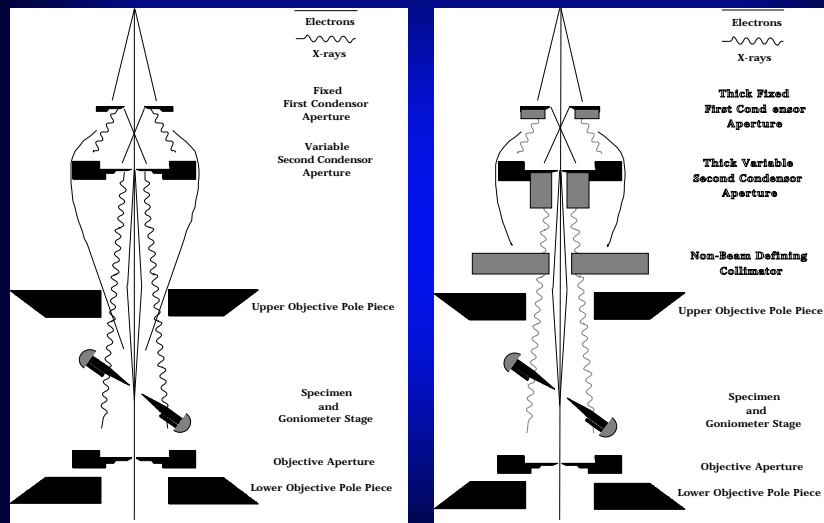
Uncollimated Radiation: The Hole Count
Effects of Thickness & Composition of Variable C2 Aperture
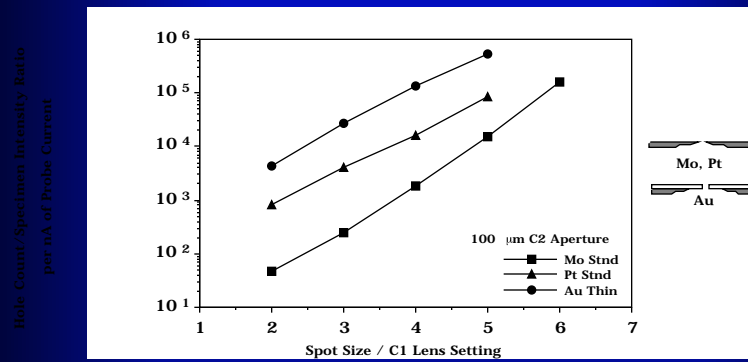
Spectral Artifacts in the AEM

Specimen: 200 Å Molybdenum Film on Holey Carbon supported on a Stnd Mo Aperture with 200 μm hole. Expt. Conditions: 120 kV, Specimen tilted toward Si(Li) 35 degrees.
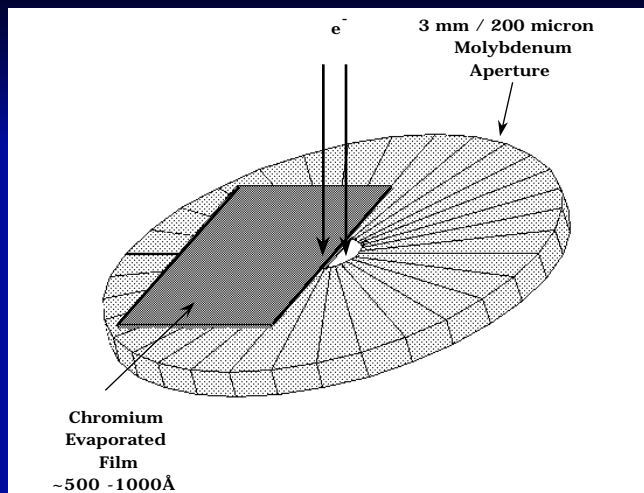
Spectral Artifacts in the AEM

Hole Count Effects: Modified C_1 and C_2 Apertures
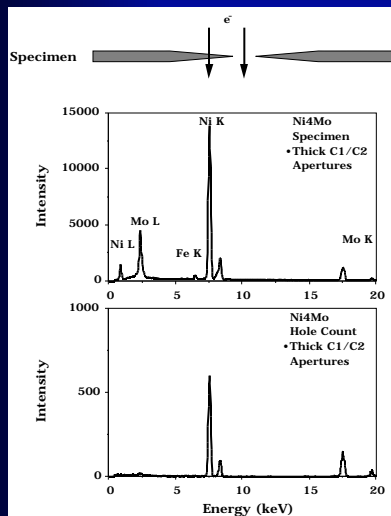
Hole Count Effects: Modified C_1 and C_2 & Non-Beam Defining Apertures
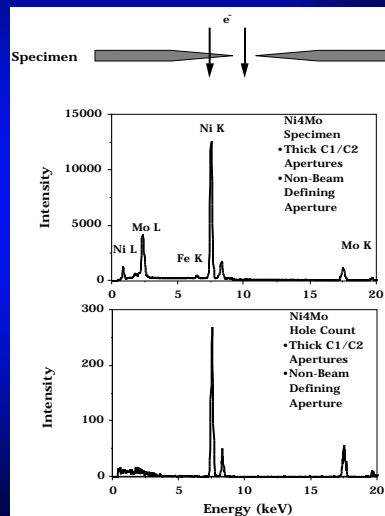
AEM/XEDS Hole Count Test Specimen

3 mm / 200 micron Molybdenum Aperture

Chromium Evaporated Film ~500 -1000Å

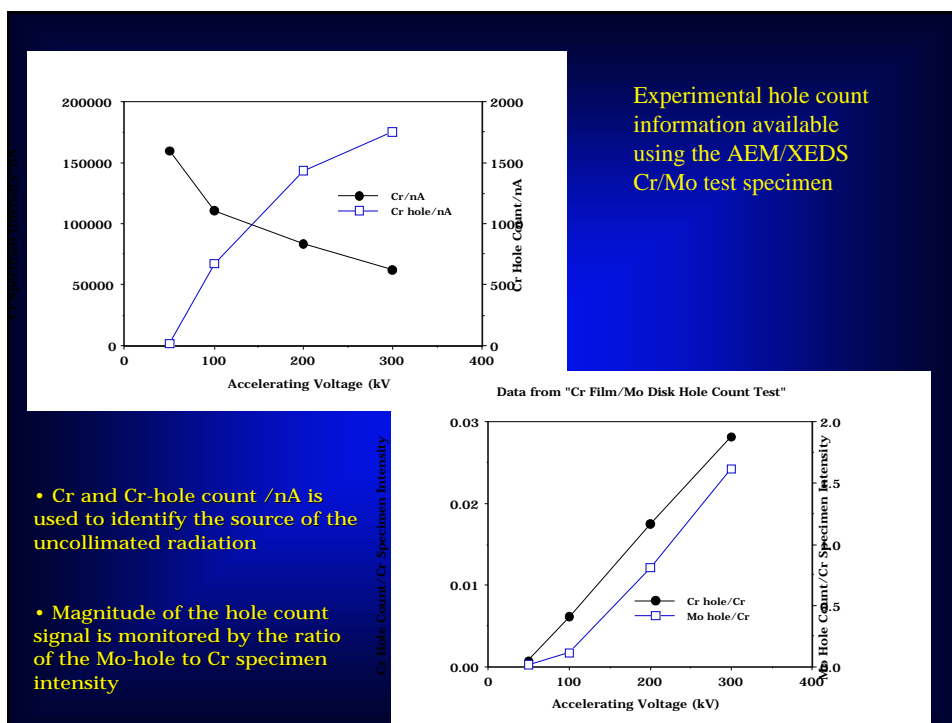**1989 Higgs Meeting XEDS/AEM Performance Panel Members**

Bentley -Oak Ridge Nat. Lab
Cazaux - UFR Sciences
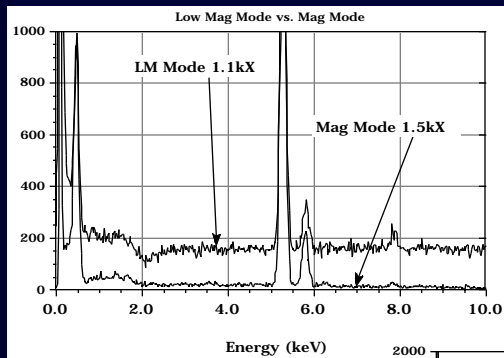Craven - Univ. of Glasgow
Glas-Lab. de Bagneux
Hren-NC State Univ.

Kruit-Delft Univ.
Malisl-PMRL/CANMET
Rez-ASU
Williams-Lehigh Univ.
Zaluzec-Argonne Nat. Lab.
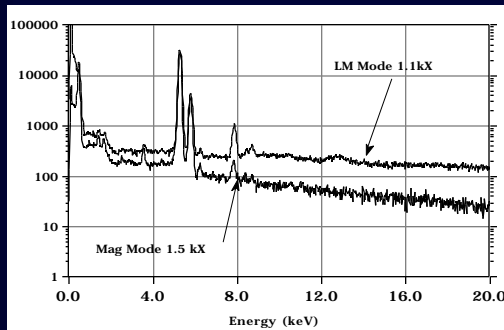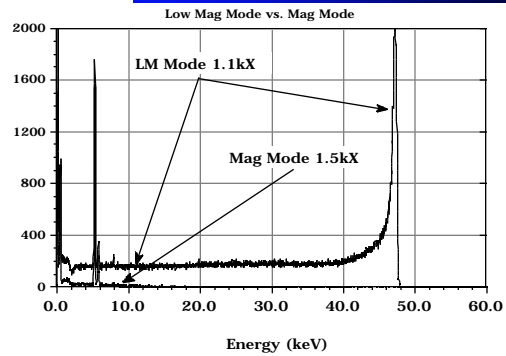
Spectral Artifacts in the AEM

Specimen Count: Chromium Film on Molybdenum Disk

Hole Count - Chromium Film on Molybdenum Disk
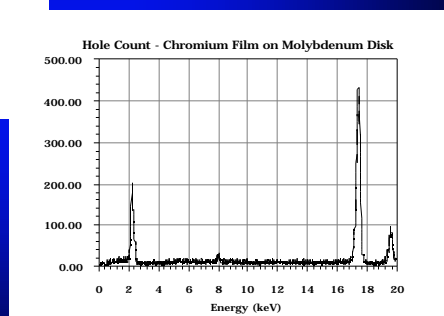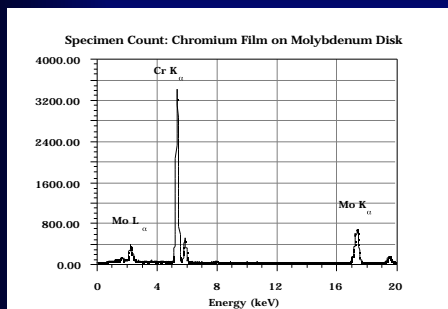
Examples of X-ray Spectra from the AEM / XEDS Cr/Mo test specimen
a) beam on the specimen, b.) beam in the "hole".

Experimental hole count information available using the AEM/XEDS Cr/Mo test specimen

• Cr and Cr-hole count /nA is used to identify the source of the uncollimated radiation

• Magnitude of the hole count signal is monitored by the ratio of the Mo-hole to Cr specimen intensity

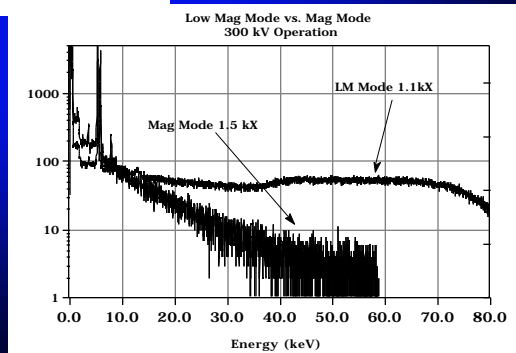**Data from "Cr Film/Mo Disk Hole Count Test"**

24

Spectral Artifacts in the AEM:
Electrons Entering the Detector
50 kV

Note the Effects of 50 keV Electrons Entering the Detector on Background

Spectral Artifacts in the AEM:
Electrons Entering the Detector
300 kV

Note the Effects of 300 keV Electrons Entering the Detector on Background

Optimizing Experimental Conditions

Choice of X-ray Line
        K- series
        L- series
        M- series

Detector/Specimen Geometry
        Elevation Angle
        Solid Angle

Detector Collimation

Choice of Accelerating Voltage
        Relative Intensity
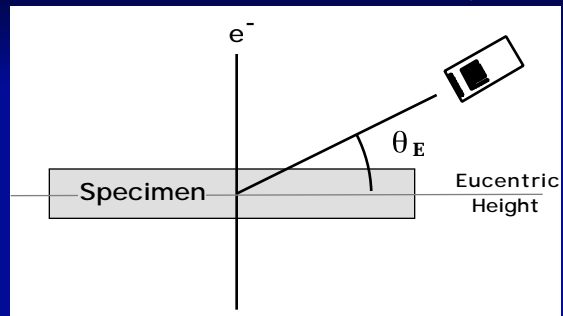   Peak/ Background
        Systems Peaks/Uncollimated Radiation

Choice of Electron Source
        Spatial Resolution
        Tungsten Hairpin
        LaB_6
        Field Emission

Radiative Partition Function (Γ) Governs the Relative Intensities
Nominal Values (Varies slowly with Atomic Number)

K Shell	L Shell	M Shell
$K_{\alpha 1} = 100$	$L_{\alpha 1} = 100$	$M_{\alpha 12} = 100$
$K_{\alpha 2} = 50$	$L_{\alpha 2} = 50$	$M_{\beta} = 60$
$K_{\beta 1} = 15\text{-}30$	$L_{\beta 1} = 50$	
$K_{\beta 2} = 1\text{-}10$	$L_{\beta 2} = 20$	
$K_{\beta 3} = 6\text{-}15$	$L_{\beta 3} = 1\text{-}6$	
	$L_{\beta 4} = 3\text{-}5$	
	$L_{\gamma 1} = 1\text{-}10$	
	$L_{\gamma 3} = 0.5\text{-}2$	
	$L_{\eta} = 1$	
	$L_{1} = 1\text{-}3$	

Detector/Specimen Geometry

Designation	Elevation Angle θ_E	Azimuthal Angle θ_A	Manufacturer
Low	0°	45°	JEOL
	0°	90°	JEOL, Philips, VG
Intermediate	15-30°	90°	Philips, JEOL, Hitachi, VG
High	68-72°	0°	Hitachi, JEOL

Detector/Specimen Geometry

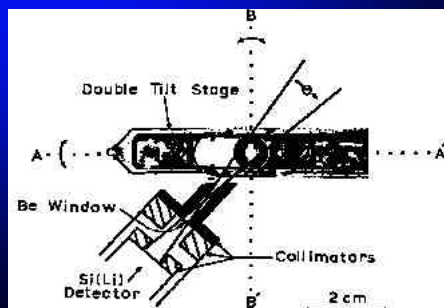## Detector/Specimen Geometry
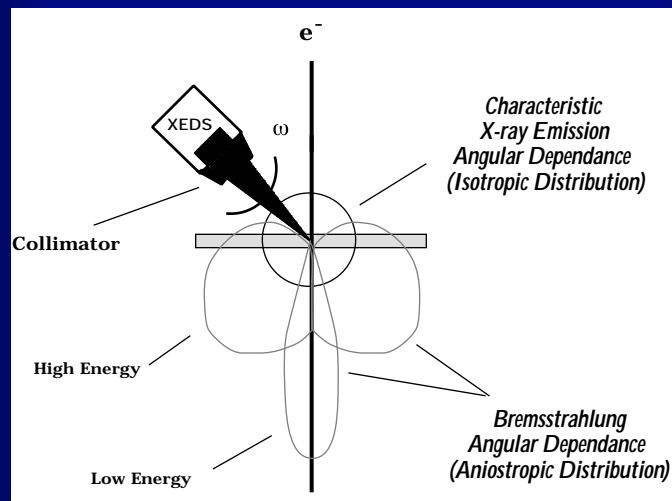
Subtending Solid Angle

Collection Solid Angle

$\omega = A/R^2 = 0.3 - 0.001$ sR
A = Detector Active Area
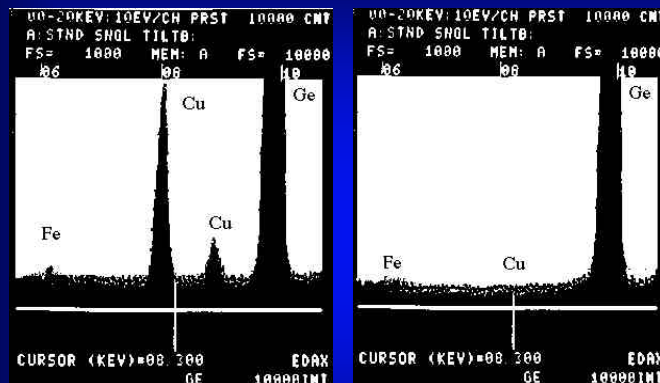= 10-30 mm2
R = Crystal to Specimen Distance
= 10 - 50 mm
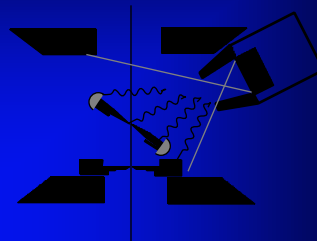
Detection of System Peaks
Effects of the Collimator & Stage

Detection & Removal of System Peaks



Removal of Stage System Peaks by use of Beryllium Gimbals
Ge specimen 10,000 in Ge K peak in both spectra
Left Standard Single Tilt Cu Stage, Right Be Gimbal DT Stage

Reactive Gas Plasma Processing
Applications to Analytical Electron Microscopy

Example:

- *The figure at the right shows the results of contamination formed when a 300 kV probe is focussed on the surface of a freshly electropolished 304 SS TEM specimen.*

- *The dark deposits mainly consist of hydrocarbons which diffuse across the surface of the specimen to the immediate vicinity of the electron probe. The amount of the contamination is a function of the time spent at each location. Here the time was varied from 15 - 300 seconds.*
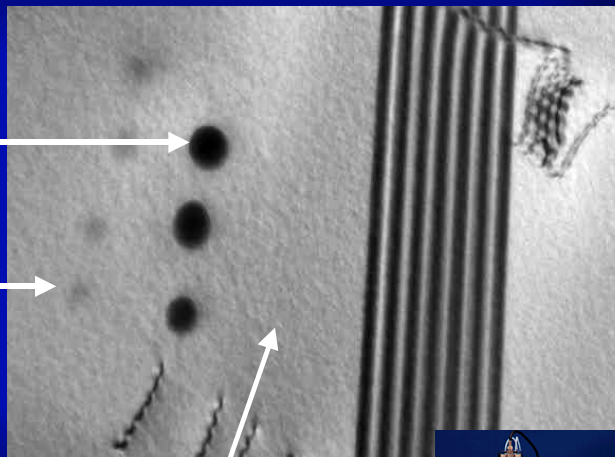

15 sec
30 sec
60 sec
120 sec
300 sec
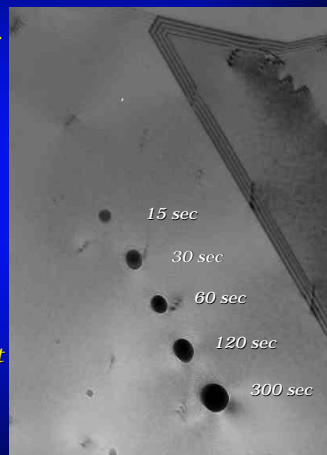
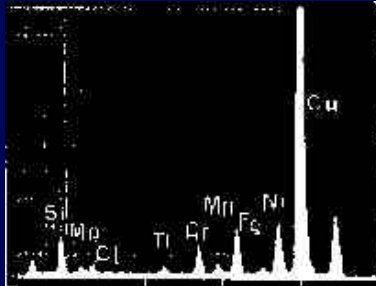## Comparision Results on Electropolished 304 SS

- **Untreated Specimen**
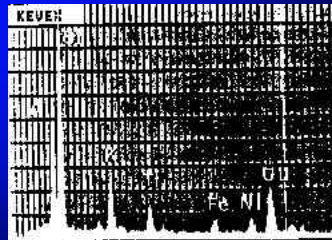
- **After 5 minutes Argon Processing**

- **After 5 minutes of additional Oxygen Processing**

Specimen Contamination Effects

Electropolishing leaves residual Cl on surface

Ion Milling leaves redeposited Fe, Ni, Cu from SS Holder & Cu Washer

---

X-ray Production = Cross-section * electrons

Maximizing The Signal

η = Probe current $= \dfrac{(\pi d_0 \alpha_0)^2 \, \mathcal{B}}{4}$

$\mathcal{B}$ = Brightness $= (\dfrac{J_c}{\pi kT}) eV_r$

V_r = Relativistic Voltage $= V_0(1 + \dfrac{eV_0}{[\ 2m_0c^2\ ]})$

$V_0(1 + 9.785 \times 10^{-7} V_0)$
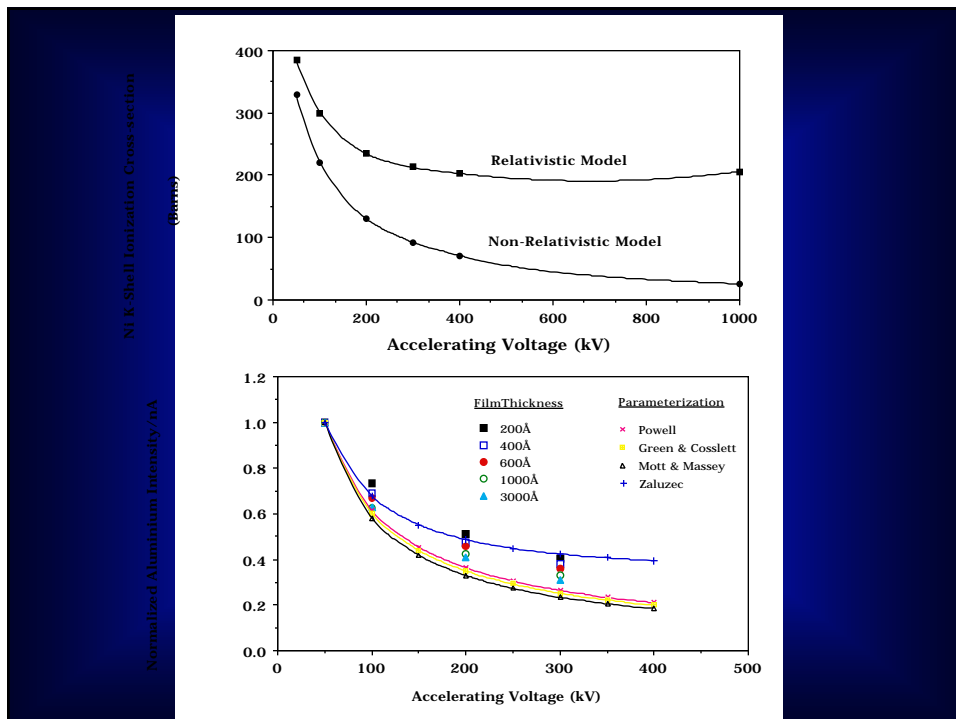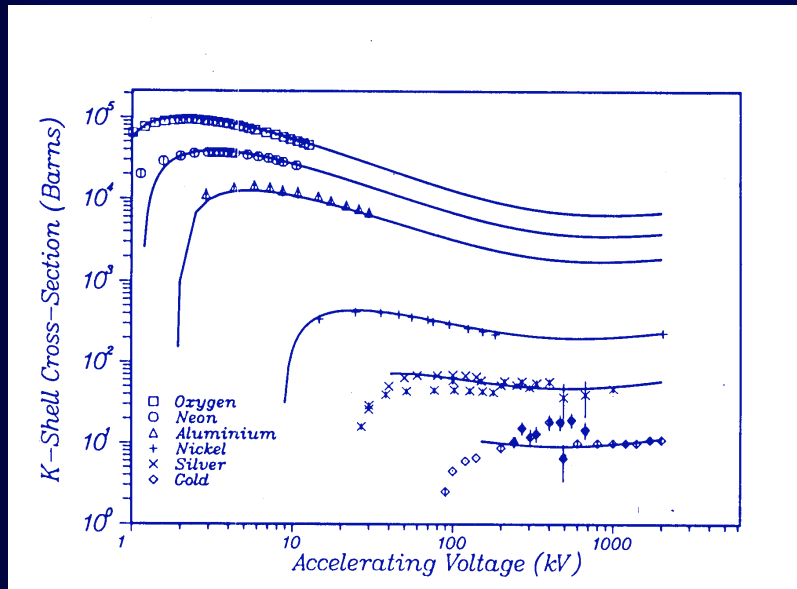
Non-Relativistic Cross-section Model

$Q_K = \dfrac{a_K * b_K * \{\ \ln\ (c_K * \dfrac{E_O}{E_C})\}}{E_O \ E_C}$

Relativistic Cross-section Model

$Q_K = \dfrac{a_K * b_K * \{\ \ln\ (c_K * \dfrac{T_O}{E_C}) - \ln(1-\beta^2) - \beta^2\}}{T_O * E_C}$

$T_O = 1/2\ m_0 c^2 \beta^2$, where $\beta = v/c$

30

Effects on Intensity with Accelerating Voltage for constant Probe size parameters
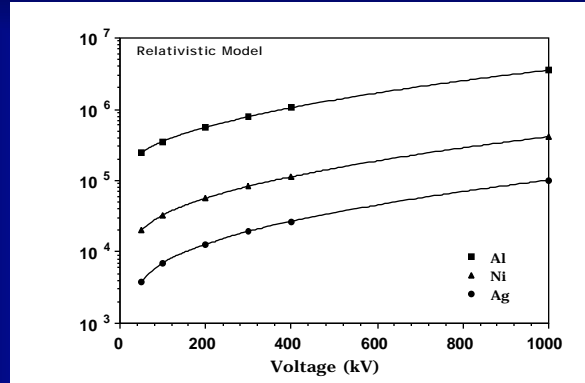
$$I = Q * \eta$$

For identical probe diameters one has higher x-ray production at higher voltage due to the increase in beam current.
Alternatively, one can achieve the same statistical intensity for smaller probes at higher

Experimental Variation of Beam Current and X-ray Intensity with Voltage
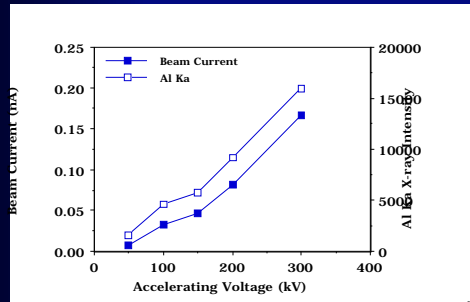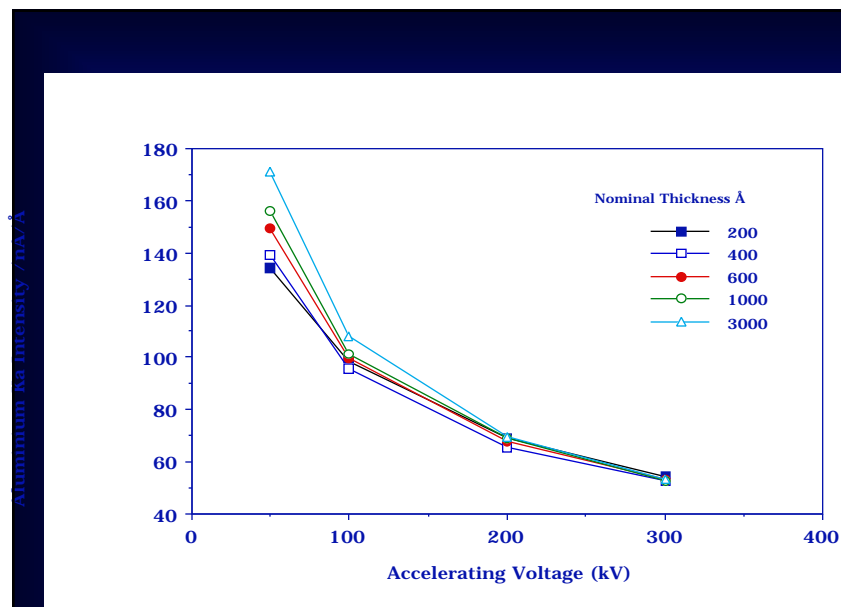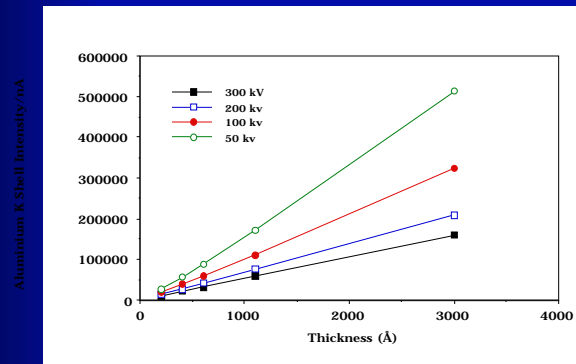
Al K intensity/na/Å as a function of accelerating voltage for different specimen thicknesses.

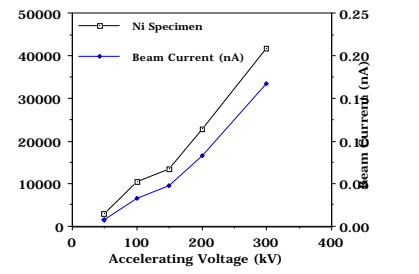## Minimium Detectable Mass

$$MDM \sim \frac{k}{P_X I_o T} = \frac{k^*}{P_X J_o d_o^2 T} \quad -$$

Minimum Mass Fraction

$$MMF \sim \frac{k}{\sqrt{[P_X (\frac{P}{B})_X I_o T]}} = \frac{k^*}{\sqrt{[P_X (\frac{P}{B})_X J_o d_o^2 T]}}$$

$k, k^* = $ Constants

$P_x = $ Characteristic Signal from element X

$(P/B)_x = $ Peak to Background ratio for element X

$I_o = $ Incident electron flux

$J_o = $ Incident electron current density

$d_o = $ Probe diameter

$T = $ Analysis time

Experimental Peak/Background Variation with Voltage

Normalized Peak/Background Ratio

3

2

1

0

● Germanium
▲ Chromium
■ Aluminium

0   100   200   300   400
Accelerating Voltage (kV)

Aluminium Peak to Background Ratio

120
110
100
90
80
70
60
50
40
30
20
10
0

□ Al P/B 400Å
□ Al P/B 1200Å
○ Al P/B 3000Å

0   100   200   300   400
Accelerating Voltage (kV)
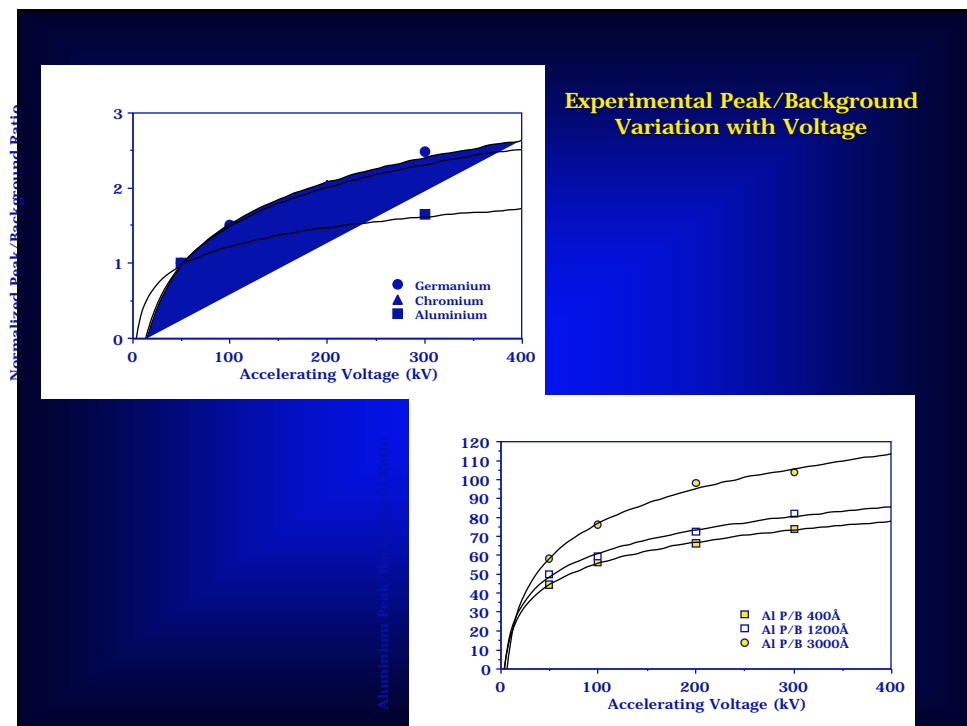
		Current	**Future**
XEDS			
	Sensitivity	MMF~10^{-3}	~10^{-4}
		MDM~10^{-20}	~10^{-22}
	Quantification	2-10% same	
	Instrumentation	Si(Li),HPGe	Si(Li),HPGe, UTW, WL
	Limitations	Radiation Damage	
EELS			
	Sensitiviity	MMF~10^{-4}	~10^{-5}
		MDM~10^{-22}	~10^{-24}
	Quantification	10-20% same	
	Instrumentation	Serial/Parallel	
	Limitations	Radiation Damage	
Future Directions	Electronic/Atomic Structure		

Spatial Resolution /Beam Spreading Monte Carlo Calculations

DC Joy's MC Program
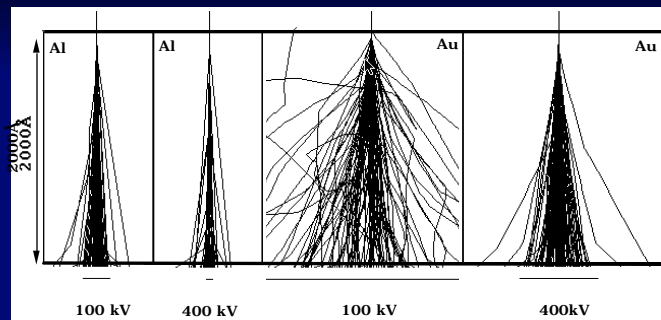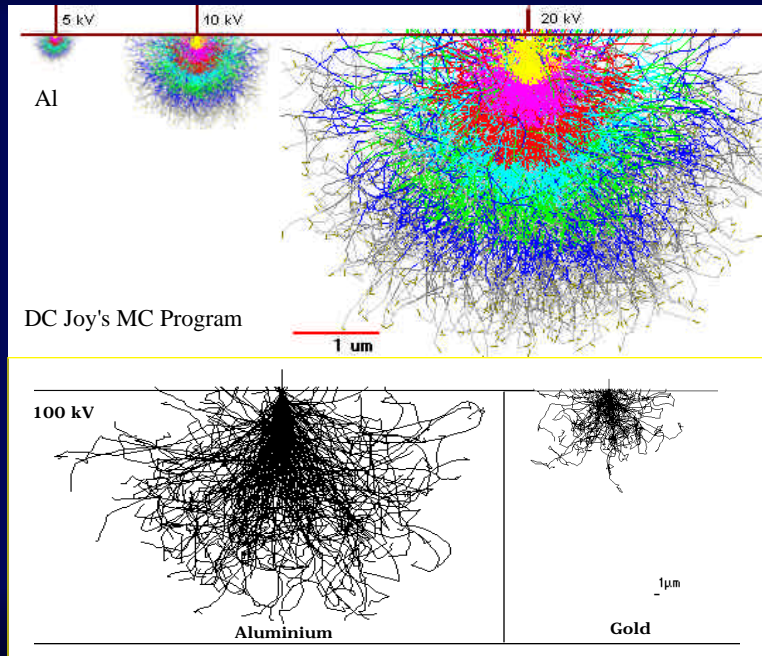
Monte Carlo Calculations of _B_ (Newbury & Myklebust -1979)

| | | | Thickness | | |
Element	Z	10nm	50nm	100nm	500nm
Carbon	6	0.22	1.9	4.1	33.0
Aluminium	13	0.41	3.0	7.6	66.4
Copper	29	0.78	5.8	17.5	244.0
Gold	79	1.71	15.0	52.2	1725.0

Analytic Formulation (Elastic Scattering - Goldstein etal 1977)

$$\mathcal{B} = 625 \frac{Z}{E_0} \sqrt{\frac{\rho}{A}} \, t^{3/2}$$
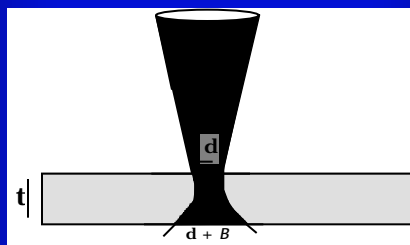
b = Beam Broadening [cm]   Z= Atomic Number
E_0= Accelerating Voltage [kV] ρ = Density [gms/cm³]
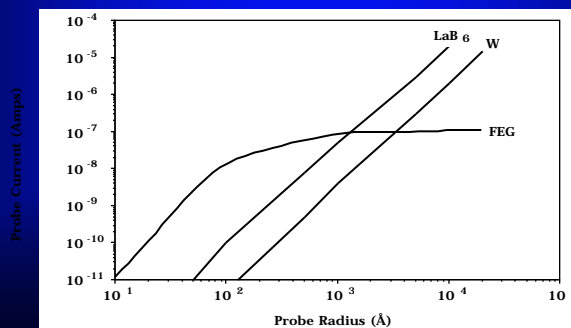A= Atomic Weight   t = Thickness [cm]

Element	Z	10nm	50nm	100nm	500nm
Carbon	6	0.16	1.8	5.13	57.4
Aluminium	13	0.26	1.9	8.12	90.9
Copper	29	0.68	7.6	21.4	*
Gold	79	15.5	17.3	*	*

*model invalid at higher kV and/or high scattering angles

Comparison of Electron Sources

| Type		Brightness β/Vo A/cm²/sr/eV	Source Size (µm)	Energy Spread (eV)	Noise	Stability	Cohereny	Vacuum (Torr)
Thermonic	Hairpin	1	50	2-3		Good	Low	$<10^{-4}$
	Pointed	5	10		Low	Fair	Moderate	$<10^{-5}$
LaB₆	Poly Crystal	10-30	10			Good	Moderate	$<10^{-6}$
	Single Crystal	20-50	5	~1	Low			
Field Emission	Thermal Assist	100-500		~.5		Moderate		$<10^{-8}$
	Cold	100-1000	<100Å	<.25	Fair	Fair	High	$<10^{-10}$

Data Analysis and Quantification:

Spectral Processing
Thin Film Quantification Methods
Specimen Thickness Effects:
    Absorption
    Fluorescence

Spectral Processing : XEDS

Spectrum = Characteristic Peaks + Background
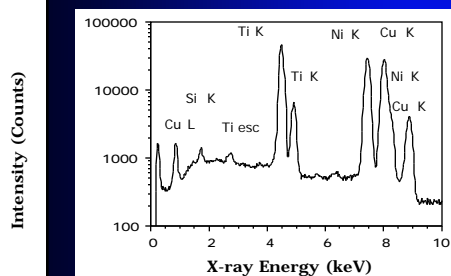
Data Reduction

Simple: Linear Background Fit & Integration

Curve Fitting: Non-Linear Background & Profile Matching

Frequency (Digital) Filtering: Background Suppression & Reference Spectra Fitting
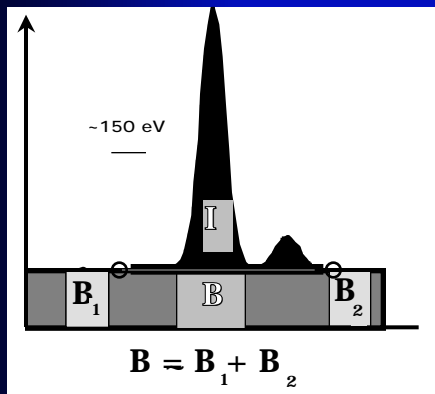
Deconvolution : Fourier Method for Resolution Enhancement

Background Modeling

Simple - Linear and/or Polynominal Interpolation

Modeling - Parametric Fits of Analytic Expressions
    Phenomenological Expressions
    Modified Bethe Heitler Model
    Digital Filtering - Mathematical Supression

Spectral Processing : XEDS
Simple Data Reduction

Note: Must use peak integrals (I) and not peak amplitudes (A)

Recall that for a Gaussian Peak

$$I = \int_{-\infty}^{+\infty} A \exp\left(\frac{-x^2}{2\sigma^2}\right) dx = \sqrt{2\pi}\,\sigma\, A$$

Hence for the ratio of Intensities

$$\frac{I_1}{I_2} = \frac{\sigma_1 * A_1}{\sigma_2 * A_2} \neq \frac{A_1}{A_2}$$
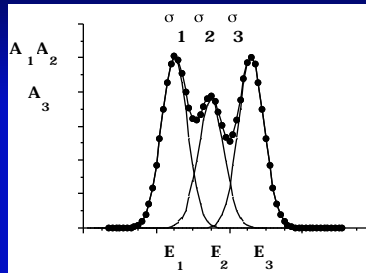
$$B = B_1 + B_2$$

Spectral Processing : XEDS

Background Modeling : Power Law/Parametric Fits

$$Bgnd = \varepsilon * \left[A\left(\frac{E-E_o}{E}\right)^2 + B\left(\frac{E-E_o}{E}\right) + C \right]$$

Slide 1
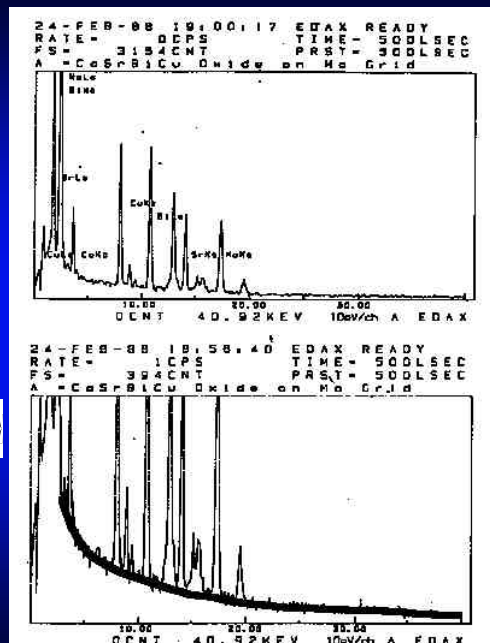
Spectral Processing : XEDS
Curve Fitting : Linear Modeling

Let

$$G_{ij} = \exp\left(\frac{-(E_j - E_i)^2}{2\sigma_{Ei}^2} \right)$$

then

$$Y_1 = A_1 \ast G_{11} + A_2 \ast G_{21} + A_3 \ast G_{31}$$
$$Y_2 = A_1 \ast G_{12} + A_2 \ast G_{22} + A_3 \ast G_{32}$$
$$Y_3 = A_1 \ast G_{13} + A_2 \ast G_{23} + A_3 \ast G_{33}$$

Using simple matrix algebra solve for A

• Fast and simple procedure

• Presumes operator knows all elements present

* System must be calibrated
(i.e. E_c and σ_E must be accurately known)

Slide 2

Spectral Processing : XEDS
Curve Fitting : Linear Modeling
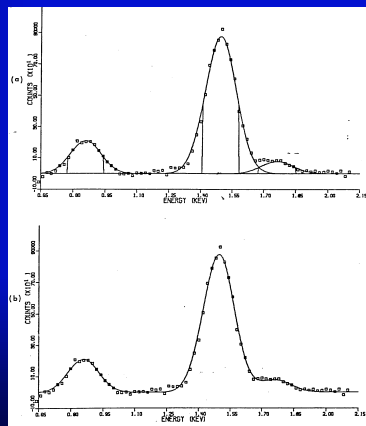
Spectral Processing : XEDS
Curve Fitting : Non- Linear Modeling

Calculate and Minimize χ^2

$$\chi^2 = \sum_{k=1}^{M}\left(\sum_{i=1}^{N} \frac{(y_i - \Upsilon_k)^2}{y_i^2}\right) \quad \text{with} \quad \Upsilon_k = A_k \exp\left(\frac{-(E_i - E_k)^2}{2\sigma^2(E_k)}\right)$$

and y_i = raw data

χ^2 is minimized by searching (E, σ, A) parameter space

Pattern Search
    - Sequential method: mechanical iteration of each parameter until a local minmimum is found.

    - Simplex method: simultaneous variation of all parameters.

Gradient Search
    - Evaluate
Multiple Least Squares with Derivitive Reference

    - Linearization of the above problem.
        E——> E + δE σ—> σ + $\delta\sigma$

$$I'(E) = I(E) - \delta E \frac{\delta I(E)}{\delta E} + \left(\sigma\delta\sigma + \frac{(\delta E)^2}{2}\right)\frac{\delta^2 I(E)}{\delta E^2}$$
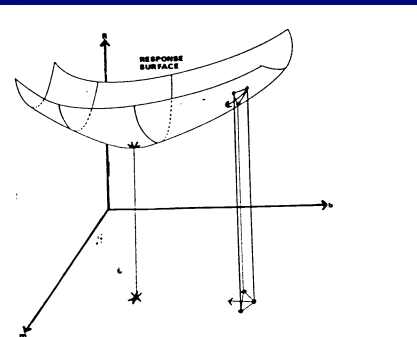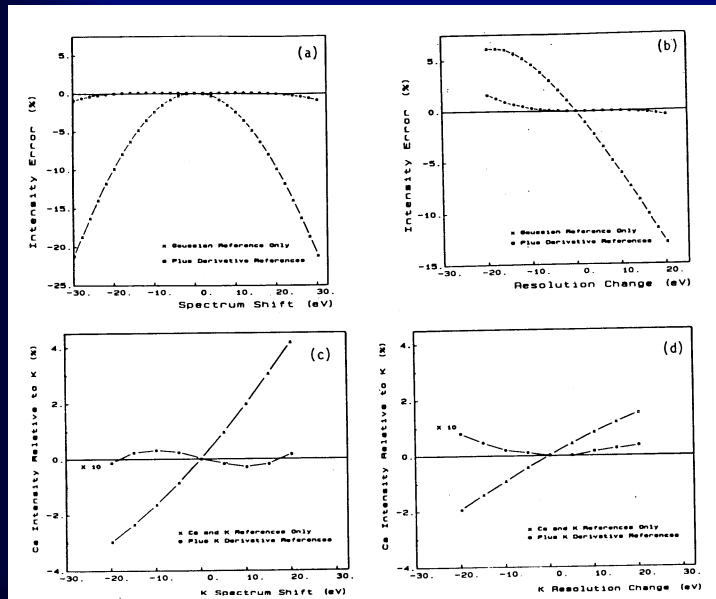

Figure 2. (m,b) plane and response surface showing a single, arbitrary, simplex.

Simplex search of Parameter Space after Fiori, NBS Special Pub. 604, 1979

**Multiple Least Squares with Derivitive Reference
Minimizes Errors due to Calibration Drift**

McMillian etal -
MAS 1984

**Spectral Processing : XEDS
Digital Filtering**

**Background Suppression by Mathematical modeling
- Replace Data by new spectra formed by the
following linear operation.**

$$G(x_i) = [F(x_{+1}) - 2*(\frac{W_-}{W_+})* F(x_0) + F(x_{-1})] \quad \text{where } F(x_j) = \Sigma f(x_j)$$

First Order (Top Hat) Digital Filter
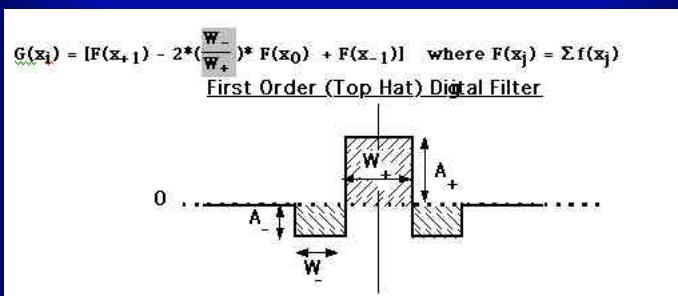
**Operator independent
Introduces severe spectral distortion**

Spectral Processing : XEDS
Digital Filtering

Original Spectrum

Ti

Ni

Cu

CuAl

Digitally Filtered

0   Energy (keV)   10

X-ray Production

X-rays Detected = X-rays Emitted * Efficiency of Collection * Efficiency of Detection
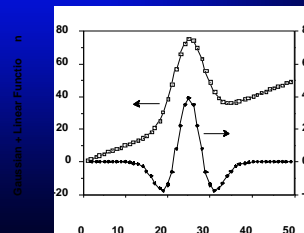
X-rays Generated * Fraction of X-rays which leave Specimen

X-rays Generated per Atom per Electron * Number of Incident Electrons * Number of Atoms * 1 + Fraction Generated by Secondary Sources

Number of "K" Shell Ionizations per Atom per Electron * Number of "K" X-rays per Ionization * Fraction of Total "K" X-rays Measured

Quantitative Analysis using XEDS

For a thin specimen

$$I_A^{K\alpha} = \left\{\sigma_A(E,Z)\Gamma_A\omega_A\right\}C_A\left\{\frac{N_o\rho}{W_A}\right\}\left\{\eta_o\ t\right\}\left\{\varepsilon_A\ \Omega\right\}$$

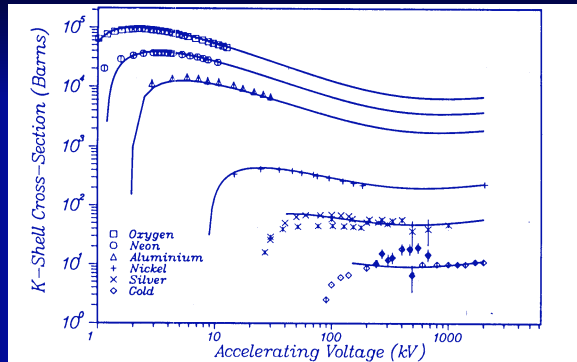|		
I_A	=	Measured x-ray intensity per unit area
	=	K^{th}-shell ionization cross-section
	=	K^{th}-shell fluorescence yield
	=	K^{th}-shell radiative partition function
W	=	Atomic Weight
N_o	=	Avagodro's number
	=	Density
C	=	Composition (At %)
$_o$	=	Incident electron flux
t	=	Specimen thickness
	=	Detector efficiency
	=	Detector solid angle

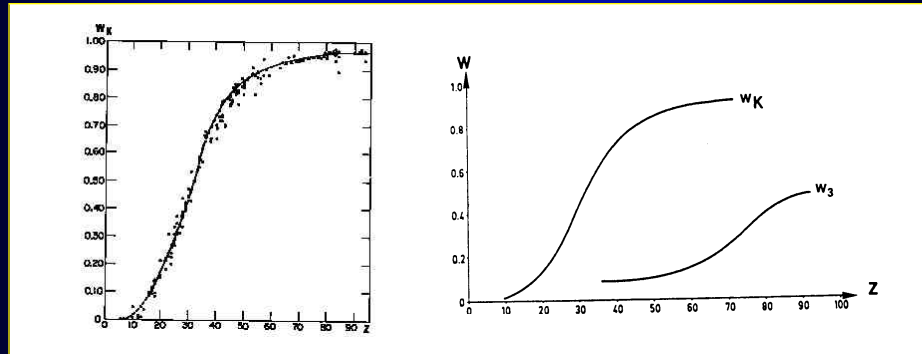
Ionization Cross-Section

For K Shells

$$Q_K = \frac{a_K \ast b_K \ast \left\{\ \ln\ (c_K \ast\frac{T_o}{E_c}) - \ln(1-\beta^2) - \beta^2\right\}}{T_o \ast E_c}$$

$T_o = 1/2\ m_o c^2\beta^2, \quad E_c = $ Shell Excitation Energy, $\quad \beta = v/c$

For L Shells

$$Q_L = \frac{a_L \ast b_L \ast \left\{\ \ln\ (c_L \ast\frac{T_o}{E_c}) - \ln(1-\beta^2) - \beta^2\right\}}{T_o \ast E_c}$$

X-ray Fluorescence Yield has Systematic Variation With Atomic Number

$_K$ shell

$_K$ vs $_L$ shell

Relative Intensities of Major X-ray Lines

$$I_K = I_{K\alpha} + I_{K\beta}$$
$$I_L = I_{L\alpha} + I_{L\beta} + I_{L\iota} + I_{L\eta} + I_{L\gamma}$$
$$I_M = I_{M\alpha} + I_{M\beta}$$

Line	Initial	Final	Line	Initial	Final	Line	Initial	Final
$K_{\alpha1}$ =>	L_3	K	$L_{\alpha1}$ =>	M_5	L_3	$M_{\alpha1}$ =>	N_7	M_5
$K_{\alpha2}$ =>	L_2	K	$L_{\alpha2}$ =>	M_4	L_3	$M_{\alpha2}$ =>	N_6	M_5
$K_{\beta1}$ =>	M_3	K	$L_{\beta1}$ =>	M_4	L_2	M_β =>	N_6	M_4
$K_{\beta2}$ =>	N_2	K	$L_{\beta2}$ =>	N_5	L_3	M_γ =>	N_5	M_3
$K_{\beta3}$ =>	M_2	K	$L_{\beta3}$ =>	M_3	L_1			
			$L_{\beta4}$ =>	M_2	L_1			
			$L_{\gamma1}$ =>	N_4	L_2			
			$L_{\gamma3}$ =>	N_3	L_1			
			L_η =>	M_1	L_2			
			L_ι =>	M_1	L_3			

Radiative Partition Function (Γ) Governs the Relative Intensities
Nominal Values (Varies slowly with Atomic Number)

K Shell	L Shell	M Shell
$K_{\alpha 1} = 100$	$L_{\alpha 1} = 100$	$M_{\alpha 12} = 100$
$K_{\alpha 2} = 50$	$L_{\alpha 2} = 50$	$M_{\beta} = 60$
$K_{\beta 1} = 15\text{-}30$	$L_{\beta 1} = 50$	
$K_{\beta 2} = 1\text{-}10$	$L_{\beta 2} = 20$	
$K_{\beta 3} = 6\text{-}15$	$L_{\beta 3} = 1\text{-}6$	
	$L_{\beta 4} = 3\text{-}5$	
	$L_{\gamma 1} = 1\text{-}10$	
	$L_{\gamma 3} = 0.5\text{-}2$	
	$L_{\eta} = 1$	
	$L_{\iota} = 1\text{-}3$	

Special Considerations for L Intensity Calculations:

$I(L\alpha) = \Gamma_{L3}(\alpha) \cdot \omega_{L3} \cdot Q_{L3}$

$I(L\beta) = \Gamma_{L3}(\beta 2) \cdot \omega_{L3} \cdot Q_{L3} + \Gamma_{L2}(\beta 1) \cdot \omega_{L2} \cdot Q_{L2} + \Gamma_{L1}(\beta 34) \cdot \omega_{L1} \cdot Q_{L1}$

$I(L\iota) = \Gamma_{L3}(\iota) \cdot \omega_{L3} \cdot Q_{L3}$

$I(L\eta) = \Gamma_{L2}(\eta) \cdot \omega_{L2} \cdot Q_{L2}$

$I(L\gamma) = \Gamma_{L2}(\gamma 1) \cdot \omega_{L2} \cdot Q_{L2} + \Gamma_{L1}(\gamma 3) \cdot \omega_{L1} \cdot Q_{L1}$

The cross-sections used should also include
Coster-Kronig Transitions (F) and K Shell Vacancies (N)

$Q_{L3}^{Total} = Q_{L3} + F_{L23} * Q_{L2} + (F_{L13} + F_{L12} \cdot F_{L23}) * Q_{L1} + N_{KL3} Q_{K}$

$Q_{L2}^{Total} = Q_{L2} + F_{L12} * Q_{L1} + N_{KL2} Q_{K}$

$Q_{L1}^{Total} = Q_{L1} + F_{KL1} Q_{K}$

Coster-Kronig Transitions:

This is an inverse transition where electrons travel up the potential well
from a lower energy state to a higher one.

K Shell Vacancies:

Generation of a K-shell X-ray results from L shell electron dropping down to the K shell and an L-shell Vacancy is created. This will lead to a indirect emission of an L shell X-ray even though the L shell core hole was not initially created by direct electron excitation.

Quantitative Analysis using XEDS
Standardless Method

**Invoke the Intensity Ratio Method, that is consider the ratio of x-ray lines from two**

$$\frac{I_A}{I_B} = \frac{\kappa_A \; \epsilon_A \; C_A}{\kappa_B \; \epsilon_B \; C_B} = k_{AB}^{-1} \frac{C_A}{C_B}$$

$$\kappa_A = \frac{\sigma_A \omega_A \Gamma_A}{W_A}$$

$$\frac{\kappa_A \; \epsilon_A}{\kappa_B \; \epsilon_B} = k_{AB}^{-1} \quad (k\text{-factor})$$

This simple equation states that the relative intensity ratio of any two characteristic x-ray lines is directly proportional to the relative composition ratio of their elemental components multiplied by some "constants" and is independent of thickness.

NOTE: The k_{AB} factor is not a universal constant!!
Only the ratio of k_A/k_B is a true physical constant and is independant of the AEM system. The ratio of e_A/e_B is not a constant since no two detectors are identical over their entire operational range. This can cause problems in some cases as we shall see.

47
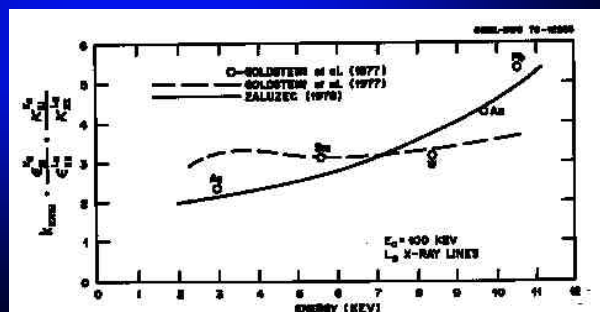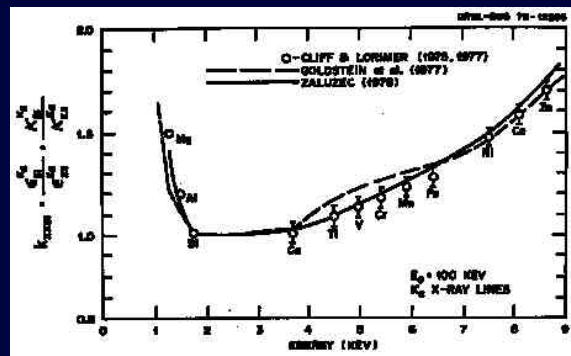
The analysis to this point has only yielded the **relative compositions** of the specimen. We need one additional assumption to convert the relative intensity ratio's (I_i/I_j) into compositons namely:

$$\sum_{i=1}^{N} C_i = 1.0$$

One now has a set of N equations and N unknowns which be solved algebraically solved for the individual composition values.

Thus for a simple two element system we have:

and
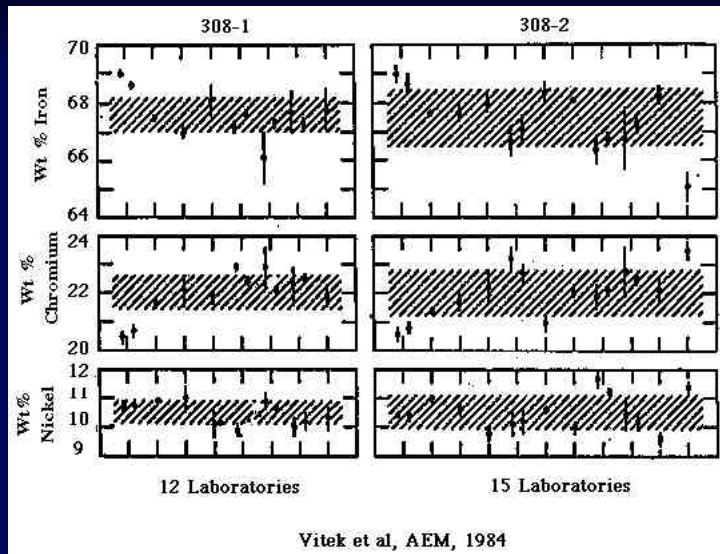
$$\frac{I_A}{I_B} = k_{AB}^{-1} \frac{C_A}{C_B}$$

$$C_A + C_B = 1.$$

or

$$C_B \left(\frac{C_A}{C_B} + 1\right) = 1$$

Soving for C_B and C_A

$$C_B = \left(\frac{1}{\left(1 + \frac{C_A}{C_B}\right)}\right) = \left(\frac{1}{\left(1 + \frac{I_A}{I_B} * k_{AB}\right)}\right) \text{ and } C_A = C_B - 1$$
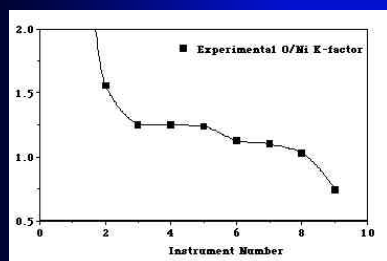

Vitek et al, AEM, 1984

Variation in Measured Composition on 308 SS for Different Labs

Example in which K-factor is stable
Cr, Fe, Ni
Note: Detector efficiency ~ 100% in this energy range

Variation in K-factor with AEM/Detector System
**Specimen: Uniform NiO film on Be Grid**

Instrument	Experimental K -Factor	Apparent Variation in Composition
1	5.17	80.9/19.1
2	1.56	56.1/43.9
3	1.25	50.6/49.4
4	1.25	50.6/49.4
5	1.24	50.4/49.5
6	1.13	48.1/51.9
7	1.10	47.4/52.6
8	1.03	45.8/54.2
9	0.74	37.8/62.2

From: Comparison of UTW/WL X-ray Detectors on TEM/STEMs and STEMs

Thomas, Charlot, Franti, Garratt-Reed, Goodhew, Joy, Lee, Ng, Plicta, Zaluzec.
Analytical Electron Microscopy-1984

Variation in K-factor with AEM/Detector System

Low Energy End will not be the only problematic area

Variation in Nominal 3 mm Si(Li) Detector Thickness
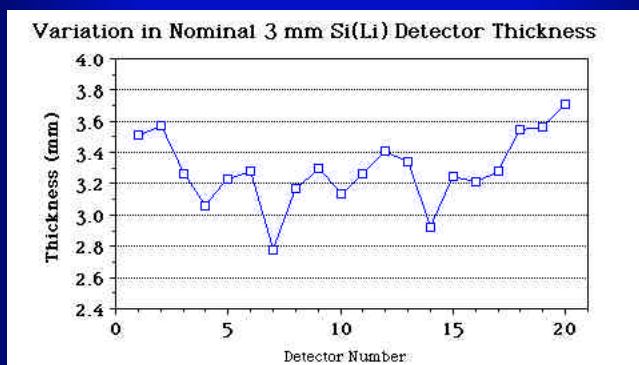
Determining the k_{AB}^{-1} **Factor**

Experimental Measurements

Prepare thin-film standards of known composition
then measure relative intensities and solve explicitly
for the k_{AB} factor needed. Prepare a working data base.

This is the "best" method, but
- specimen composition must be verified independently
- must have a standard for every element to be studied

Theoretical Calculations

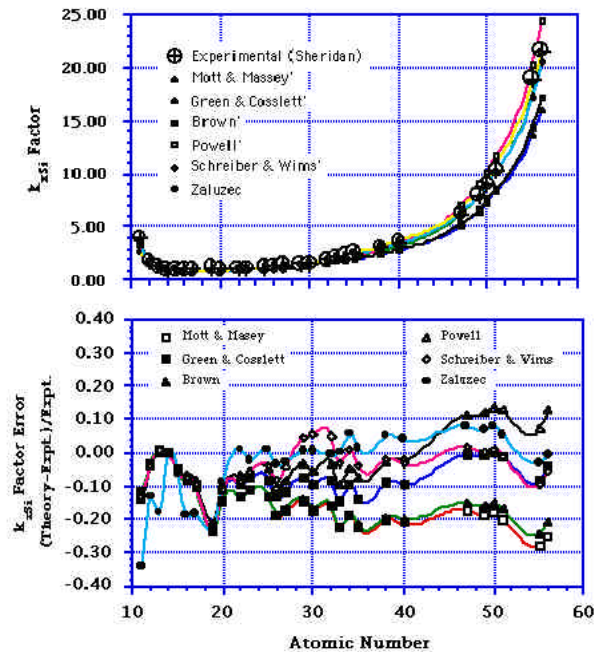Attempt first principles calculation knowing
some fundamental parameters of the AEM system
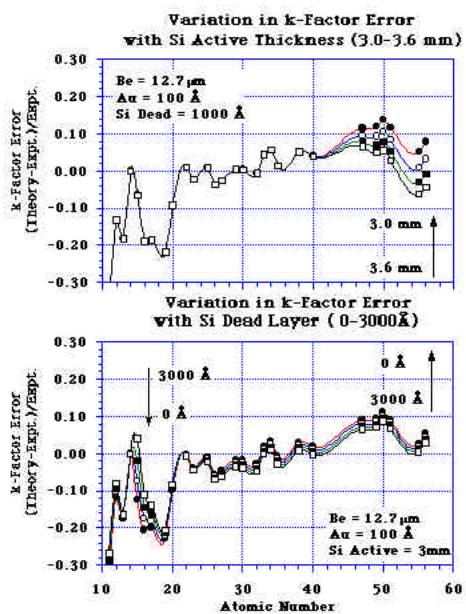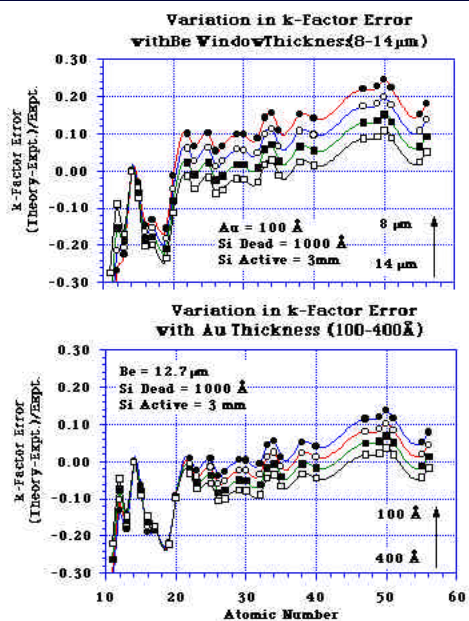
Start with a limited number of kAB factor measurements,
then fit the AEM parameters to best match the data.
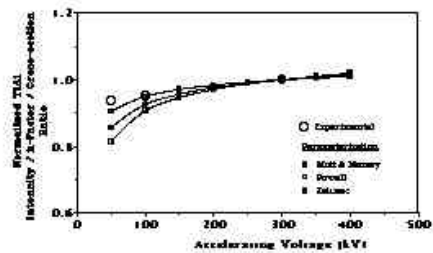Extrapolate to systems where measurements and/or
standards do not exist.

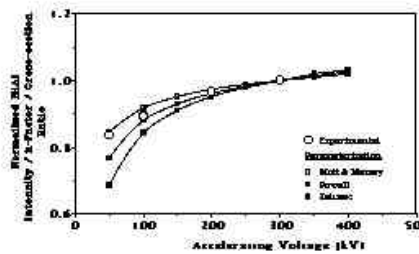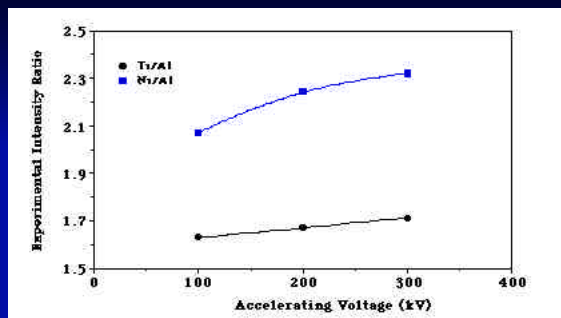**Method 1**. (Goldstein etal) Assume values for , , and determine the best s to fit k_{AB}. This
procedure essentially iterates the fit of s to the data.

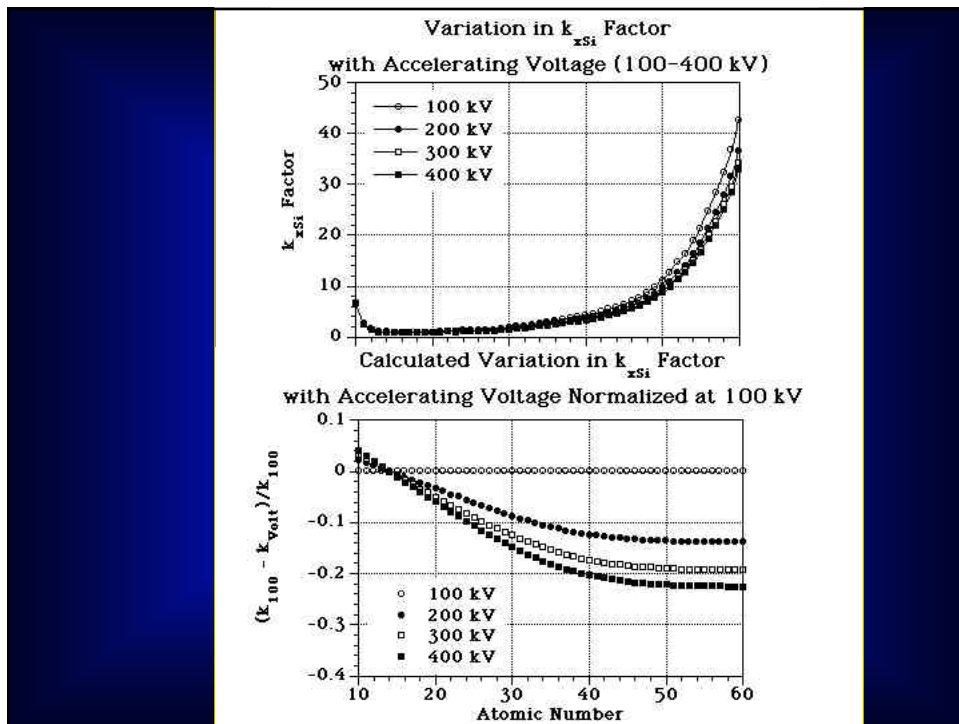**Method 2.** (Zaluzec) Assume values for , , determine the best e to fit k_{AB}. This
procedure essentially iterates the fit of e (detector window parameters) to the data.

K-Factor Calculation
Experiment
vs
Theory

Variation in k_{xSi} Factor with Accelerating Voltage (100-400 kV)

Calculated Variation in k_{xSi} Factor with Accelerating Voltage Normalized at 100 kV

Sources of values for k$_{AB}$ Calculations

W — **International Tables of Atomic Weights**

Γ(K) — **Schreiber and Wims , X-ray Spectroscopy (1982)**
Vol 11, p. 42

Γ(L) — **Scofield, Atomic and Nuclear Data Tables (1974)**
Vol 14, #2, p. 121

ω (K) - **Bambynek etal, Rev. Mod. Physics, Vol 44, p. 716**
Freund, X-ray Spectrometry, (1975) Vol 4, p.90

ω(L) — **Krause, J. Phys. Chem. Ref. Data (1974) Vol 8,**
p.307

σ(Eo) — **Inokuti, Rev. Mod. Physics, 43, No. 3, 297 (1971)**
- Goldstein etal, SEM 1, 315, (1977)
- Chapman etal, X-ray Spectrometry, 12,153,(1983)
- Rez, X-ray Spectrometry, 13, 55, (1984)
- Egerton, Ultramicroscopy, 4, 169, (1969)
- Zaluzec, AEM-1984, San Fran. Press. 279, (1984)

ε (E) — **Use mass absorption coefficients from:**
-Thinh and Leroux; X-ray Spect. (1979), 8, p. 963
-Henke and Ebsiu, Adv. in X-ray Analysis,17, (1974)
-Holton and Zaluzec, AEM-1984, San Fran Press,353,(1984)

Quantitative Analysis using XEDS
Thin Film Standards Method

Invoke the Intensity Ratio Method, but now consider the ratio of the same x-ray line from two different specimens, where one is from a **standard** of known composition while the other is **unknown**:

$$\frac{I_u}{I_s} = \frac{\eta_u}{\eta_s} \, \frac{\rho_u}{\rho_s} \, \frac{t_u}{t_s} * \frac{C_u}{C_s}$$

$$C_u = \frac{\eta_s}{\eta_u} \, \frac{\rho_s}{\rho_u} \, \frac{t_s}{t_u} * \frac{I_u}{I_s} * C_s$$

This simple equation states that the relative intensity ratio of same characteristic x-ray line is directly proportional to the relative composition ratio of the two specimens multiplied by a some new parameters.

η = **incident beam current**
ρ = **local specimen density**
t = **local specimen thickness**

Quantitative Analysis using XEDS
Specimen Thickness Effects

For finite thickness specimens, what is a thin film?

Previous Assumptions:
        No Energy loss,
        No X-ray absorption,
        No X-ray fluorescence

NOTE: Electron Transparency is insufficient!

Effects of energy loss on Characteristic X-ray Production:

$$I_A = \frac{N_O \; \rho \; C_A}{W_A} \; \omega_A \Gamma_A \; \eta_o \; \Omega \; \varepsilon_A \int_o^{t_o} \sigma_A(E) \; dt$$

$$I_A = \frac{N_O \; \rho \; C_A}{W_A} \; \omega_A \Gamma_A \; \eta_o \; \Omega \; \varepsilon_A \int_o^{t_o} \sigma_A(E) \; dt$$

Calculated Change in σ with Energy Loss

$$\frac{\Delta\sigma}{\sigma} = \frac{\sigma(100) - \sigma(100 - \Delta E)}{\sigma(100)}$$

Energy Loss(eV)	Al	Ni	Ag
500	0.004	0.003	0.002
1000	0.009	0.006	0.004
2000	0.018	0.013	0.009
5000	0.047	0.030	0.022

Quantitative Analysis using XEDS
Specimen Thickness Effects

Consider the mean energy loss of a electron beam () going through a film of thickness = "t". Let s = electron pathlength (~thickness) then (Inokuti -1971):

$$\frac{dE}{ds} = \frac{\pi e^4 N_o \rho Z}{WE} \left\{ \ln\left(\frac{2ET_E}{J^2(1-\beta^2)}\right) - 2\ln(2)\sqrt{(1-\beta^2)} \right.$$

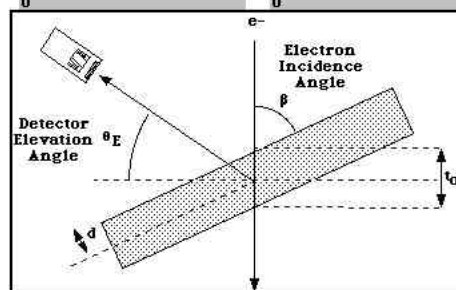$$\left. + 1-\beta^2 + \frac{(1-\sqrt{1-\beta^2})^2}{8} \right\}$$

Calculated Energy Losses (eV) as a function of pathlength

Voltage	Pathlength	Al	Ni
100 kV	100 nm	87	255
	400 nm	349	1020
300 kV	100 nm	51	150
	400 nm	203	60

For conventional specimen thicknesses used in AEM, the effect of energy loss on characteristic x-ray production is negligible.

Quantitative Analysis using XEDS : Absorption Correction

$$I = \int_0^{t_o} I_o(t)\,\exp(-\mu^* d)\,dt = \int_0^{t_o} I_o(t)\,\exp(-\chi \rho t)\,dt$$

e−

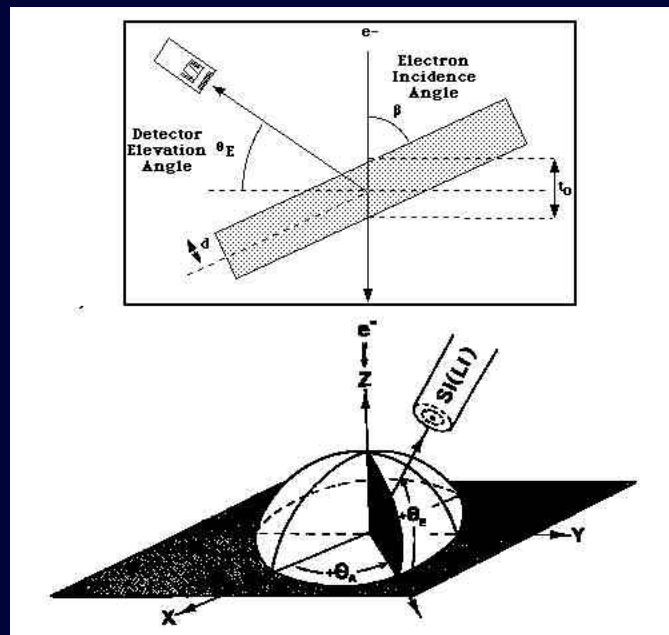Electron Incidence Angle β

Detector Elevation Angle θ_E

t_o

d

d = Absorption Pathlength from the specimen to detector

$$= t\,\frac{\sin(\beta)}{\cos(\beta-\theta_E)}$$

χ = Geometrical factor multiplied by average mass absorption coefficient for the measured x-ray line in the compound

$$= \left(\frac{\mu}{\rho}\right)_{\text{Spec.}}^{\text{x in}} * \frac{\sin(\beta)}{\cos(\beta-\theta_E)}$$

$\left(\frac{\mu}{\rho}\right)_{\text{Spec.}}^{\text{x in}}$ = Weighted average mass absorption coefficient

$$= \sum_{i=1}^{N} \left(\frac{\mu}{\rho}\right)_i * C_i \quad \text{(Note: composition dependent!)}$$

$$\beta = \text{Arccos} \left(\frac{\sin\phi_y \cdot \cos\theta_A \cdot \cos\theta_E \ + \ \sin\phi_x \cdot \cos\phi_y \cdot \cos\theta_E \cdot \sin\theta_A}{\sqrt{a^2+b^2+c^2}} \right)$$

$a = \cos\phi_x \cdot \cos\phi_y \cdot \cos\theta_A \cdot \cos\theta_E$

$b = \cos\phi_x \cdot \cos\phi_y \cdot \cos\theta_E \cdot \sin\theta_A$

$c = \sin\phi_y \cdot \cos\theta_A \cdot \cos\theta_E + \sin\phi_x \cdot \cos\phi_y \cdot \cos\theta_E \cdot \sin\theta_A$

Now rederive the standardless equations to include absorption.

$$\frac{I_A}{I_B} = \frac{\varepsilon_A}{\varepsilon_B} * \frac{\kappa_A}{\kappa_B} * \frac{\delta_A}{\delta_B} * \frac{C_A}{C_B}$$

with

$$\frac{\delta_A}{\delta_B} = \frac{\left(\frac{\mu}{\rho}\right)^{B\ in}_{AB}}{\left(\frac{\mu}{\rho}\right)^{A\ in}_{AB}} \frac{\left(1-\ \exp(-\chi\rho t^*)^{A\ in}_{AB}\right)}{\left(1-\ \exp(-\chi\rho t^*)^{B\ in}_{AB}\right)}$$

$$t^* = t_o\ \frac{\sin(\beta)}{\cos(\beta-\theta_E)}$$

$$\chi = \left(\frac{\mu}{\rho}\right)^{X\text{-}ray\ in}_{Compound} = \sum_{i=1}^{N}\left(\frac{\mu}{\rho}\right)_i * C_i$$
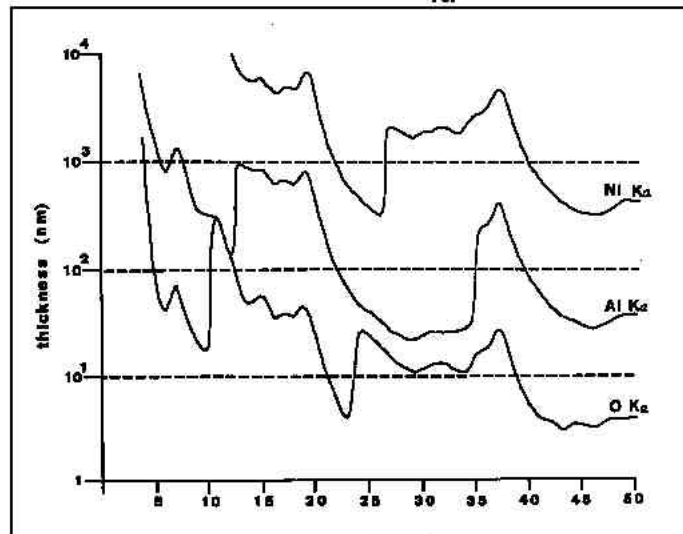
β = Electron Incidence Angle

= Function of Stage Tilts: ϕ_x, ϕ_y, & Detector Azimuth θ_A)

θ_E = Detector Elevation Angle
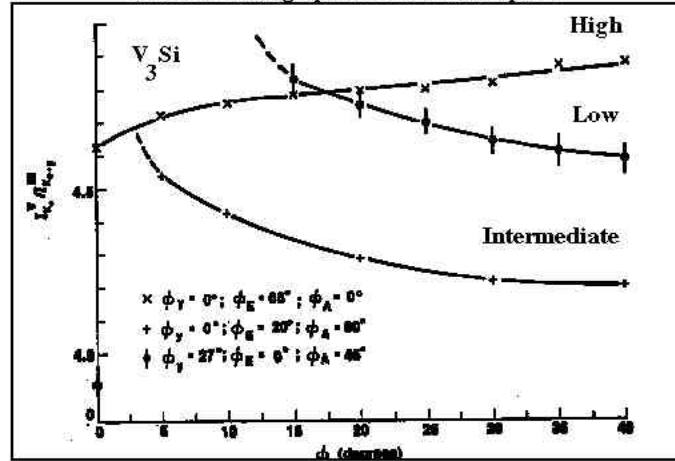
Define the Thin Film approximation: $\chi\rho t^* < 0.1$

Thin Film approximation: $\chi\rho t^* < 0.1$

$$t^* \leq \frac{0.1}{\chi\rho}$$

Effect of Tilting Specimen on Absorption

For a plane paralle slab specimen, tilting has the effect
of increasing the Specimen Thickness.
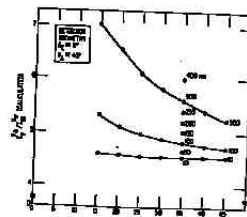Different Detector/Specimen Geometries will enhance/reduce
the Absorption Effects

FIG. 1.--Theoretically calculated intensity ratio of $I_L^{Kα}/I_{Kβ}$ as function of specimen tilt $θ_X$ at detector/specimen geometry of $θ_E = 0°$, $θ_A = 45°$ for specimen thickness values ranging from 10 to 400 nm as indicated.
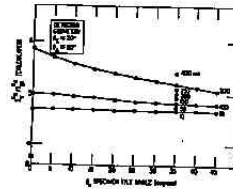
FIG. 2.--Theoretically calculated intensity ratio of $I^{Kα}/I_{Kβ}$ as function of specimen tilt $θ_X$ at detector/specimen geometry of $θ_E = 20°$, $θ_A = 90°$ for specimen thickness values ranging from 10 to 400 nm as indicated.
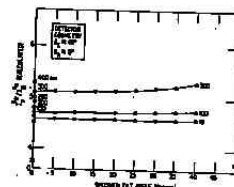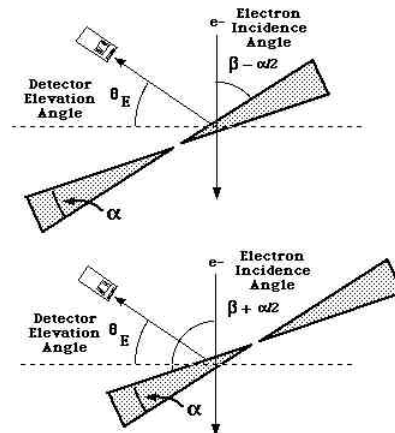
FIG. 3.--Theoretically calculated intensity ratio of $I^{Kα}/I_{Kβ}$ as function of specimen tilt $θ_X$ at detector/specimen geometry of $θ_E = 60°$, $θ_A = 0°$ for specimen thickness values ranging from 10 to 400 nm as indicated.

In the "real" world few specimens have the shape used to derive this correction. Next consider two representative geometries:

Symmetric Wedge Geometry:

Replace all β's by $\beta \pm \alpha/2$. where α is the wedge angle of the specimen
$+\alpha/2$ variant applies when the detector is positioned such that the pathlength *increases* relative to the parallel slab model
$-\alpha/2$ variant applies when the detector is positioned such that the pathlength *decreases* relative to the parallel slab model
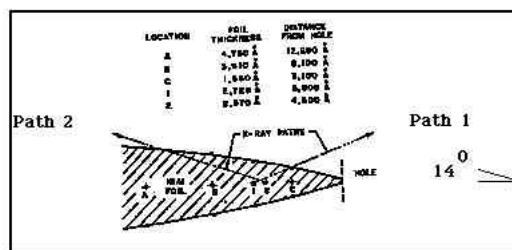
Glitz etal (MAS-1981)

Attempt a Wedge Model Correction using previous formulae.

Path #1	Path #2
$\dfrac{I_{Ni}}{I_{Al}} = 2.64$	$\dfrac{I_{Ni}}{I_{Al}} = 5.18$
Thin Film Model $\dfrac{Ni=60.9}{Al=39.1}$	Thin Film Model Error!
Parallel Slab $\dfrac{Ni=45.3}{Al=54.7}$	Parallel Slab $\dfrac{Ni=60.5}{Al=39.5}$
Wedge Model $\dfrac{Ni=50.6}{Al=49.4}$	Wedge Model $\dfrac{Ni=42.6}{Al=57.4}$
$\chi \rho t_{Ni} = 0.016$	$\chi \rho t_{Ni} = 0.081$
$\chi \rho t_{Ni} = 0.925$	$\chi \rho t_{Ni} = 4.24$

Absorption Correction has limited applications keep $\chi \rho t < 1$

Specimen Homogenity

In this and all other derivations we have assumed that over the excited volume, as well as along th exiting pathlength, the specimen is homogeneous in composition. If this assumption is invalid, one must reformulate the absorption correction and take into account changes in : $\mu/$, , and t along the exiting pathlength.

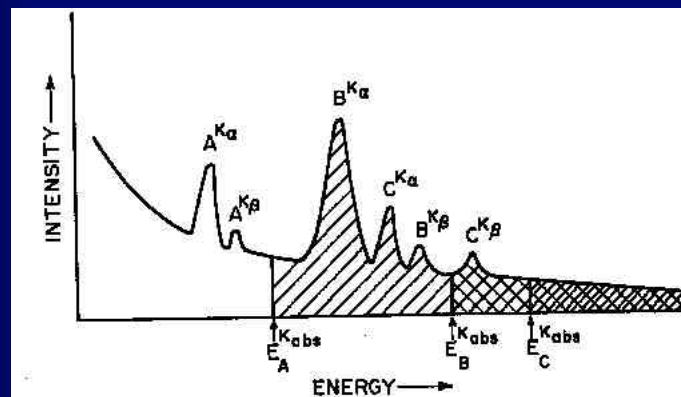**Effects of Beam Broadening**

Parallel Slab Model: No Change in absorption pathlength
Wedge Model: There is a correction the magnitude of which varies with the wedge angle.

Effects of Irregular Surface

This cannot be analytically modeled but must be understood!
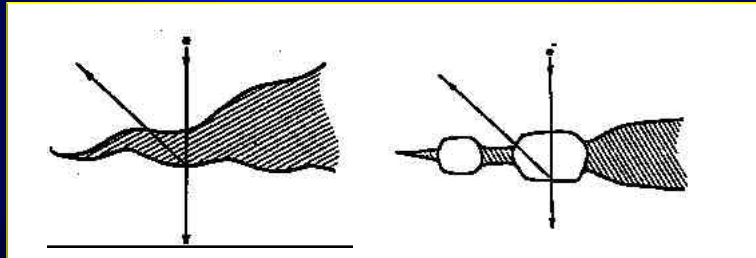
X-Ray Fluorescence Correction

$$I_A^{Measured} = I_A^{Electron} + I_A^{XRF\ by\ B}$$

$$I_A^{Measured} = I_A^{Electron} \left(1 + \frac{I_A^{XRF\ by\ B}}{I_A^{Electron}} \right) |$$

Calculation of the Intensity of I_A x-rays due to fluorescence by I_B

$$dI_A^{XRF\ by\ B} = I_B \bullet \left[\exp\left(-\left(\tfrac{\mu^B}{\rho}\right)_{AB} \rho\, z\, \csc\phi\right) \right] \bullet \left[\rho C_A \left(\tfrac{\mu^B}{\rho}\right)_A \csc(\phi) \right] \bullet \left[\left(\tfrac{\Delta\mu}{\mu}\right)_A \right] \bullet \left[\omega_A \bullet \Gamma_A \right]$$

$$dI_A^{XRF\ by\ B} = I_B \bullet P_A^{XRF\ by\ B}\, dz\, d\phi$$

$\left[\exp\left(-\left(\tfrac{\mu^B}{\rho}\right)_{AB} \rho\, z\, \csc\phi\right) \right]$ — Fraction of B x-rays that are absorbed in the material AB on leaving at angle ϕ from depth z

$\left[\rho C_A \left(\tfrac{\mu^B}{\rho}\right)_A \csc(\phi) \right]$ — Probability that B x-rays are absorbed by atoms of type A

$\left[\left(\tfrac{\Delta\mu}{\mu}\right)_A \right]$ — Probability that upon absorption the K-Shell is ionized for A

$\left[\omega_A \bullet \Gamma_A \right]$ — Probability that a $K\alpha$ x-ray is emitted

Now integrate this over the specimen geometry $\phi = 4\pi$, T=thickness

$$I_A^{XRF} = \int_0^{4\pi} \int_0^T dI_A^{XRF} = \int_0^{4\pi} \int_0^T I_B \bullet P_A^{XRF}\, dz\, d\phi$$

Substituting for I_B and dividing by I_A and generalizing to element i

$$\frac{I_A^{XRF\ by\ i}}{I_A} = C_i\ \omega_i\ \Gamma_i\ \frac{A_A}{A_i}\ \frac{Q_i}{Q_A}\left(\tfrac{\Delta\mu}{\mu}\right)_A \left(\tfrac{\mu^i}{\rho}\right)_{Ai} \int_0^{4\pi}\int_0^T (\text{terms in Exp \& } \csc\phi)\, dz\, d\phi$$

Solution depends on the geometric assumptions
(see for example Twigg & Fraser MAS, 1982)

$$\frac{I_A^{XRF\ by\ i}}{I_A} = C_i\ \omega_i\ \Gamma_i\ \frac{A_A}{A_i}\ \frac{Q_i}{Q_A}\left(\tfrac{\Delta\mu}{\mu}\right)_A \left(\tfrac{\mu^i}{\rho}\right)_A \frac{\rho T}{2}\left[1.12 + \left(\tfrac{\mu^i}{\rho}\right)_{Ai} \bullet \frac{\rho T}{4} - \ln\left(\left(\tfrac{\mu^i}{\rho}\right)_{Ai} \bullet \rho T\right) \right]$$

for a plane parallel slab specimen

Now

$$\text{Define } \gamma_A = \left(1 + \sum_{i=1}^{N} \frac{I_A^{XRF\ by\ i}}{I_A^{Electron}} \right)$$

Next rederive the standardless equations to include x-ray fluorescence and you can show.

$$\frac{I_A}{I_B} = \frac{\varepsilon_A}{\varepsilon_B} * \frac{\kappa_A}{\kappa_B} * \frac{\delta_A}{\delta_B} * \frac{\gamma_A}{\gamma_B} * \frac{C_A}{C_B}$$

as in the case of x-ray absorption this requires iterative solution because the ratio of γ's are composition dependent.

When is the XRF Correction important?

- When fluorescing line is near the absorption edge of the lower energy line. Typically within a few atomic numbers (i.e. Z+2 to Z+6)
- When specimen is thick or path length is long

Define a thin film approximation for XRF as:

$$\frac{I_A^{XRF \; by \; i}}{I_A^{Electron}} < 0.05$$

$$C_i \; \omega_i \; \Gamma i \; \frac{A_A}{A_i} \frac{Q_i}{Q_A} \left(\frac{\Delta\mu}{\mu}\right)_A \; \left(\frac{\mu^i}{\rho}\right)_A \frac{\rho T}{2} \left[1.12 + \left(\frac{\mu^i}{\rho}\right)_{A_i} \bullet \frac{\rho T}{4} - \ln\left(\left(\frac{\mu^i}{\rho}\right)_{A_i} \bullet \rho T \right) \right] < 0.05$$

Examples Absorption & Fluorescence Corrections

Assume 100 kV, $\theta_A = 90^o$, $\theta_E = 20^o$, $\beta = 35^o$, $\alpha = 0^o$ i.e. tilted parallel slab

Ni 90%, Fe 10%

Calculation of Thin Film approximation $\chi\rho t \Rightarrow 1.25\mu m$ for Fe in the Alloy

∴ for TEM specimens we can almost always ignore absorption effects

What about XRF?

Let T = 5000Å $\dfrac{I_{Fe}^{XRF \; by \; Ni}}{I_{Fe}^{Electron}} = 0.103$ i.e. ~10%

Let T = 1000Å $\dfrac{I_{Fe}^{XRF \; by \; Ni}}{I_{Fe}^{Electron}} = 0.028$ i.e. 2.8%

∴ for TEM specimens we may be affected by XRF

Ni 90%, Al 10%

Calculation of Thin Film approximation $\chi\rho t$ => 232 Å for Al in Alloy!!!

$\therefore$ for TEM specimens we cannot ignore absorption effects

What about XRF?

Let T = 5000Å $\qquad \dfrac{I_{Al}^{XRF\ by\ Ni}}{I_{Al}^{Electron}} = 0.000186$ i.e. 0.01%

$\therefore$ for typical TEM specimens we can ignore XRF effects

---

Quantitative Analysis using XEDS - Bulk

For a Bulk Specimen:

$$I_A^{K\alpha} = \left| \Gamma_A \omega_A \int_{E_c}^{E} \frac{\sigma_A(E,Z)}{S_A} dE \right| \left| R_A \right| \left| f(\chi) \right| \left| \mathcal{F}_A \right| C_A \left| \frac{N_o \rho}{W_A} \right| \eta_o \varepsilon_A \Omega$$

I_A	=	Measured x-ray intensity per unit area
σ	=	K^{th}-shell ionization cross-section
ω	=	K^{th}-shell fluorescence yield
Γ	=	K^{th}-shell radiative partition function
R	=	Backscatter Correction Term
S	=	Electron Stopping Power
$f(\chi)$	=	Absorption Correction Term
F	=	Fluorescence Correction Term
W	=	Atomic Weight
N_O	=	Avagodro's number
ρ	=	Density
C	=	Composition (At %)
η_o	=	Incident electron flux
t	=	Specimen thickness
ε	=	Detector efficiency
Ω	=	Detector solid angle

Quantitative Analysis using XEDS
Standards Method

Invoke the Intensity Ratio Method, but now consider the ratio of the same x-ray line from two different specimens, where one is from a **standard** of known composition while the other is **unknown**:

$$\frac{I_U^{K\alpha}}{I_S^{K\alpha}} = \frac{\left[\Gamma_A \omega_A \int_{E_c}^{E} \frac{\sigma_A(E,Z)}{S_U}dE\right] \left[R_U\right] \left[f_U(\chi)\right] \left[\mathcal{F}_U\right] \left[C_U \frac{N_0\rho}{W_A}\right] \eta_0 \varepsilon_A \Omega}{\left[\Gamma_A \omega_A \int_{E_c}^{E} \frac{\sigma_A(E,Z)}{S_S}dE\right] \left[R_S\right] \left[f_S(\chi)\right] \left[\mathcal{F}_S\right] \left[C_S \frac{N_0\rho}{W_A}\right] \eta_0 \varepsilon_A \Omega}$$

$$\frac{I_U^{K\alpha}}{I_S^{K\alpha}} \equiv K_{Ratio} = K_Z \bullet K_A \bullet K_F \bullet \frac{C_U}{C_S}$$

or rearranging

$$C_U = K_{Ratio} * (ZAF\ Corrections) * C_S$$

These equations state that the relative intensity ratio of same characteristic x-ray line is directly proportional to the relative composition ratio of the two specimens multiplied by a some correction terms

---

Advantages
Standard may be a pure element.
The closer the standard is to the unknown material the smaller the correction and higher the accuracy.

Disadvantages
Effects of surface films can be critical
Must have a standard for each element to be analyzed

Additional Topics

Heterogeneous Specimens
Composition Profiles
Electron Channeling
Radiation Damage

All quantitative analysis equations were derived assuming
that the specimen is homogeneous over the exited volume

Application of the these equations to heterogenous specimens
effectively averages the composition over the excited volume.
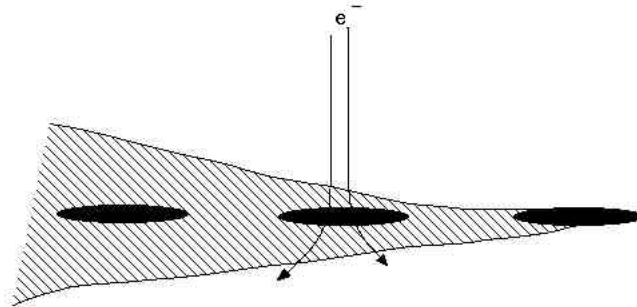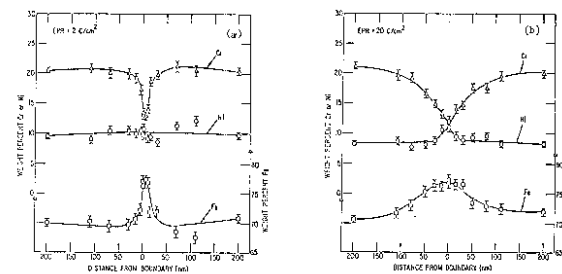
$$C^*(x,y) = C(x,y,z) * d(x,y,z)$$

$C^*(x,y)$ = Apparent profile measured
$C(x,y,z)$ = Actual composition profile
$d(x,y,z)$ = Incident beam profile

$*$ = Convolution operator

F, F^{-1} = Fourier and Inverse Fourier Transforms

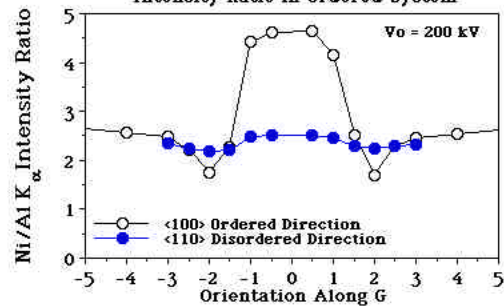In the 2 dimensional limit one can deconvolute the measured profile using:

$$C(x,y) = F^{-1}\left[\frac{F\{C^*(x,y)\}}{F\{d(x,y)\}}\right]$$

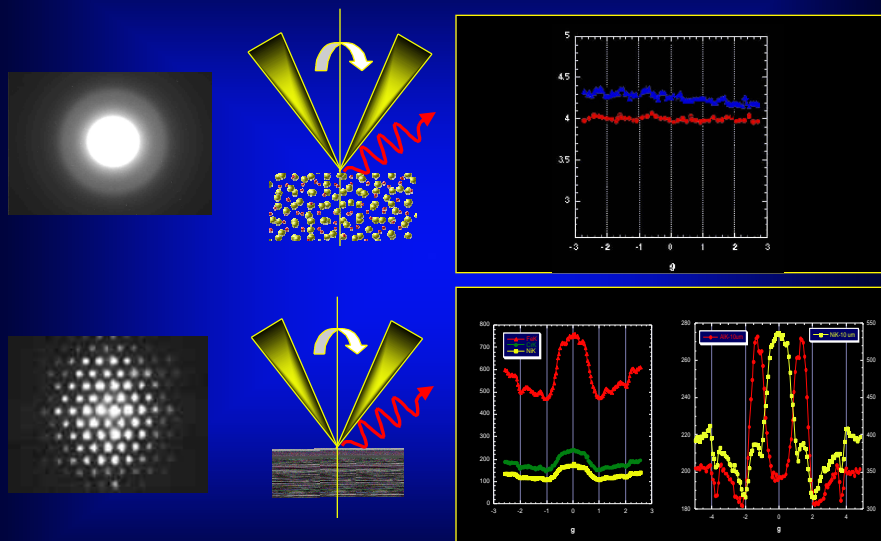Realistically, it is better to decrease the probe diameter and specimen thickness
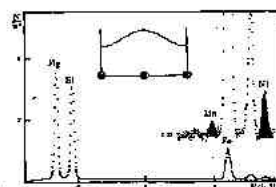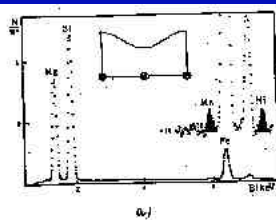
Electron Channeling Effects
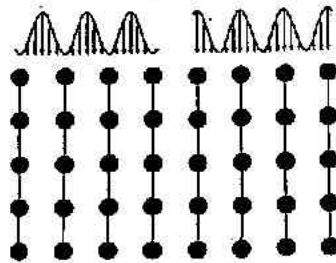
High Angular Resolution Electron Channeling X-ray Spectroscopy

ALCHEMI
Atom Location by CHanneling
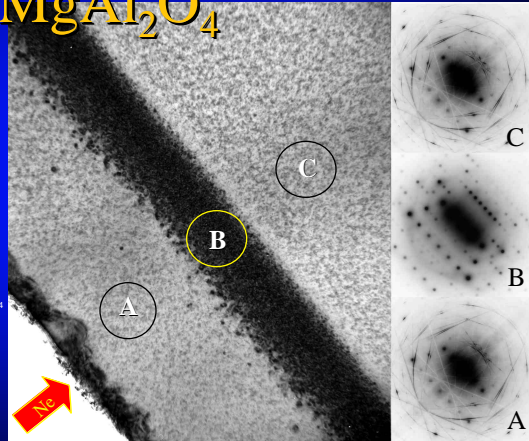**EMIssion**
Tafto & Spence - Science 1982

$(Mg_{0.90}Fe_{0.10}Ni_{0.004}Mn_{.002})_2SiO_4$
Note: Mn prefers Si Sites and Ni prefers Mg Sites

Studies of Spinel $MgAl_2O_4$

1MeV Ne into $MgAl_2O_4$
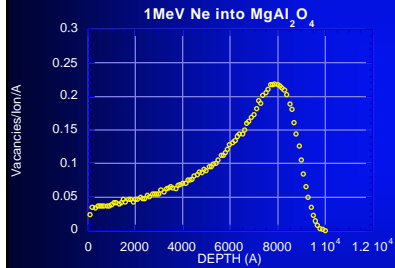
with T.Soeda, S. Matsumura, L. Rehn
Kyushu Univ. / ANL

$MgAl_2O_4$ Cross-Section

HAREC XS - $MgAl_2O_4$

Mg
Al
O

{110}

Experimental

Calculated

Unirradiated

Irradiated
1 MeV Ne
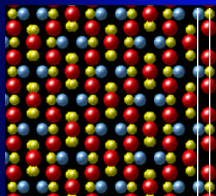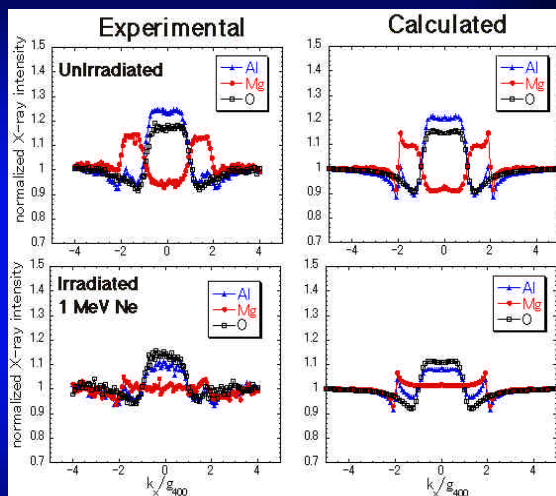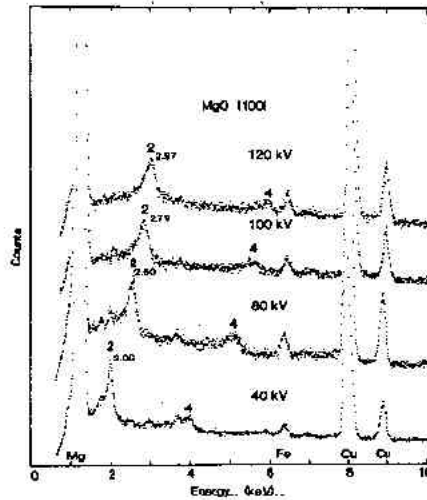
with T.Soeda, S. Matsumura, L. Rehn
Kyushu Univ. / ANL

Coherent Bremmstrahulung
Reese, Spence, and Yamamoto- Phil Mag. 1984 Vol 49, 5, 697

Radiation Damage vs Microanalysis

Comparison of Characteristic Signal Generation and Displacement Rates

$\dfrac{\text{Ionizations}}{\text{sec}}$ $\qquad N_i = Q * J * C \dfrac{N_o \rho}{A}$

$\dfrac{\text{Displacements}}{\text{sec}}$ $\qquad N_d = \sigma_d * J * \phi(f) * C \dfrac{N_o \rho}{A}$

$\dfrac{\text{Detected X-rays}}{\text{sec}}$ $\qquad N_i = Q *[\omega_X \Gamma_X \varepsilon_X \Omega_X] \, J * \, C \dfrac{N_o \rho}{A}$

$\dfrac{\text{Detected EEL}}{\text{sec}}$ $\qquad N_i = Q *[\omega_E \Gamma_E \varepsilon_E \Omega_E] \, J * C \dfrac{N_o \rho}{A}$

$\omega_E \sim \Gamma_E \sim \varepsilon_E \sim 1$

Radiation Damage vs Microanalysis

Energy Transfered by an Incident Electron to an Atomic Nucleus

$$T_T = \frac{2 * T_o * (T_o + 2 * m_o c^2) * \sin^2(\frac{\phi}{2})}{Mc^2}$$

To = eVo, M = nuclear mass, mo = electron mass, f = scattering angle

Comparison of Maximum Transferable Kinetic Energy for Selected Elements with Displacement and Sputtering Energies (all values in eV)

Element	<-------	----------	-T_T-------	---------->	$T_d{}^1$	$T_s{}^2$
	----	~	---	--->		
	100 kV	200 kV	300 kV	400 kV		
Al	8.93	19.5	31.6	45.3	16	3.5–7.0
Ti	5.00	11.0	17.8	25.5	15	4.9–9.8
V	4.73	10.3	16.72	24.0	29	5.3–10.6
Cr	4.63	10.1	16.38	23.5	21	4.1–8.2
Fe	4.31	9.40	15.25	21.8	16	4.3–8.6
Co	4.08	8.91	14.45	20.7	23	4.4–8.8
Ni	4.10	8.94	14.5	20.8	21	4.5–9.0
Cu	3.79	8.26	13.4	19.2	18	3.5–7.0
Zn	3.69	8.03	13.03	18.7	16	1.4–2.8
Nb	2.59	5.65	9.17	13.2	24	7.5–15.0
Mo	2.51	5.47	8.88	12.7	27	6.8–13.6
Ag	2.23	4.87	7.90	11.3	28	3.0–6.0
Cd	2.14	4.67	7.58	10.9	20	1.2–2.4
Ta	1.33	2.90	4.71	6.75	33	8.1–16.2
Pt	1.23	2.69	4.37	6.26	33	5.9–11.8
Au	1.22	2.67	4.32	6.2	36	3.8–7.6

Td = Displacement Threshold (Bulk) Energy
Ts = Sputtering Threshold (Surface) Energy

Calculated Sputtering Cross-Sections